공학박사 학위논문

Optimization of Sustainability in Process Design Based on Covariance Matrix Adaptation Evolution Strategy

공분산행렬 적응형 진화알고리즘을 이용한 지속 가능성 최적화를 위한 공정 설계

2014년 8월

서울대학교 대학원

화학생물공학부

김 익 현

Optimization of Sustainability in Process Design Based on Covariance Matrix Adaptation Evolution Strategy

지도 교수 윤 인 섭

이 논문을 공학박사 학위논문으로 제출함
2014년 6월

서울대학교 대학원
화학생물공학부
김 익 현

김익현의 공학박사 학위논문을 인준함
2014년 6월

위 원 장 韓宗勳 (인)

부위원장 尹寅燮 (인)

위 원 李宗珉 (인)

위 원 申東一 (인)

위 원 崔用振 (인)

Abstract

Optimization of Sustainability in Process Design Based on Covariance Matrix Adaptation Evolution Strategy

Ik Hyun Kim
School of Chemical and Biological Engineering
The Graduate School
Seoul National University

Preliminary design in chemical process furnishes economic feasibility through the calculation of both mass balance and energy balance, and it makes the process possible to produce a desired product under the given conditions. Through this design stage, the process possesses unchangeable characteristics, since the materials, reactions, unit configuration, and operating conditions are determined. Therefore, it becomes more important to design process considering sustainability.

For this reason, this thesis proposes the solution procedure to integrate sustainability into traditional process economic optimization. The process

modeling is conducted by the general-purpose sequential modular simulator employed for both convenience and reliability to analyze and design chemical process. However, using the sequential modular simulator is hard to obtain derivatives of process models for the deterministic optimization strategy, and it is also difficult to satisfy the process constraints and design specifications multidirectionally interacting with design variables. Therefore the covariance matrix adaptation evolution strategy (CMA-ES), which is a stochastic black-box optimization algorithm, is adopted to overcome these difficulties in this thesis. The CMA-ES is an improved methodology in terms of accuracy and reliability to find optimal solution in comparison with other stochastic sampling based algorithms, and it has several advantages that: 1) it has much fewer initial settings required by the user, 2) it can deal with the non-convex multimodal problem even though the problem contains discontinuous decision variables so that it solves the optimization problem which is too complicated to interpret mathematical model explicitly, and 3) it has an excellent ability to optimize the multi-variable problems. These advantages improve the performance of the solution procedure proposed in the thesis.

The proposed solution methodology for optimizing the sustainability of the process is an iterative procedure which executes the nested loop consisting of the inner loop for the process model simulation and the outer loop for the economic

and sustainability optimization. Thus, 1) the CMA-ES for finding an optimal solution with much fewer function evaluations and 2) the rejection method for avoiding the execution of simulator in case of infeasible individuals make the convergence of a nested loop faster as well as expand the searching domain economically.

The effectiveness and usefulness of the proposed solution methodology in this thesis are verified by the application to practical process design problems. At first, the most profitable operating condition of an offshore oil and gas production process is determined with the consideration of the Reid vapor pressure specification and wastewater treatment cost as an environmental aspect. Second, regarding the inherently safer design of the offshore natural gas liquefaction process which involves the risk of explosion, the quantification of an inherent explosion consequence and integration of inherent risk into economic analysis make it possible to show the numerical relation between conflicted objectives and assist a decision-making to design inherently safer process.

As a result of this thesis, the proposed methodology makes it possible to design the sustainable chemical processes. It is expected to be useful in designing the sustainable process since the sustainability factors in the process can be numerically monitored during preliminary process design stage using process

simulator. Furthermore, it contributes to decrease various uncertainties during the process lifetime and minimize the risk and further expenses regarding the economic, environmental and safety aspects.

Keyword : Sustainability, Black-box optimization, Process design, Offshore platform,

Student ID : 2009 - 30239

List of Contents

List of Tables

List of Figures

Chapter 1. Introduction

1.1 Sustainability and Design of Chemical Processes

For several decades, sustainable development is a key driver in various disciplines of chemical and energy industries. In 1987, the Brundtland Commission has reported a document entitled '*Our Common Future*' which was the first occasion to introduce the concept of sustainable development [1]. The original concept was suggested pursuing development in a way that respects both human needs and global ecosystem for future generations. Recently, as it is hard to change the patterns of human activities intentionally, most definitions of sustainability contain three major aspects; which are environmental performance, societal responsibility and economic contribution in order to pursuit the continuous growth of global industries [2-8].

A lot of corporations in the world have begun to realize that concerning for sustainability is an indicator of global superb management. According to KPMG [9] in 2013, 85% of the top 100 U.S. companies and 42% of the top 100 Korean companies published annual sustainability reports, as shown in Figure 1-1. They also take more interest in Sustainability Index (SI) such as the Dow Jones Sustainability Index which is developed to assess both general and industry-

specific criteria containing approximately 80~120 questions in terms of the economic, environmental and social aspects [10]. The three elements, which are economic, environmental and social concerns, are also evaluated in order to represent the sustainability in the process industries by the Institute of Chemical Engineers (IChemE) [8, 11], United Nations Environment Programme (UNEP) [12], U.S. Environmental Protection Agency (EPA) [7], and so on. Similarly, like as other disciplines, chemical engineering has attempted to focus on the sustainability by considering factors beyond the traditional process and product. The AIChE Institute for Sustainability has introduced SI which has the ability to represent the sustainability performance of the chemical companies in terms of strategic commitment, sustainability innovation, environmental performance, safety performance, product stewardship, social responsibility and value chain management [13]. It is a noteworthy fact that the environment and safety performance is important sustainability criteria because the chemical processes have distinct features such as inherent risk from various types of accidents and widespread damage of environment or human being as well as industry.

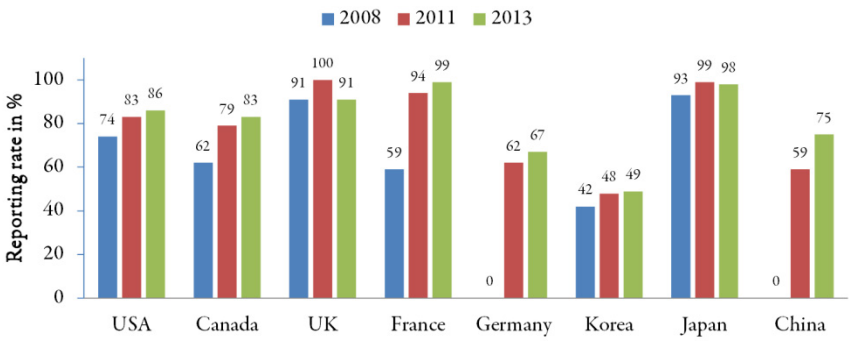

Figure 1-1Regional rate of corporate responsibility reporting

The sustainable design involves an extension of process or system boundaries to the environment, safety, and social aspect. It is also required to contemplate the quantification of sustainability over the full product and process life cycle during design and development through the integration of many disciplines including engineering, biology, economics, law, ethics, social sciences, and so on. It could assist in decision-making, guiding to integrate the evaluation of sustainability into process design rather than consider safety and environmental issues as an 'after-thought' and 'end-of-pipe'.

Traditionally, preliminary design in chemical process has been guided by economic feasibility through the calculation of both mass and energy balance, and it makes possible to produce a desired product under given conditions.

Process systems engineering has an important role in development and improvement of methods and tools to support 'decision-making for the creation and operation of the chemical supply chain with the inclusion of safety and environmental factors, as well as economics' [14]. This activity is supported by Modeling, Simulation and Optimization (MSO) tools which are developed and deployed enormously to support process design and analysis. As process systems engineers are familiar with the systematic approach in order to support their design procedure, a lot of effort is put into integrating process synthesis in MSO technology such as multi-scale modeling in the design lifecycle, linking experiments to models, sustainable process synthesis, and so on. Among these issues, sustainable process synthesis deeply involves optimization-based process synthesis [15]. Optimization-based process synthesis not only supports the evaluation of an enormous number of alternative process structures but also facilitates the integration of conflicting objectives of sustainability [16, 17].

1.2 General-Purposed Chemical Process Simulator

A general-purposed process simulator becomes more and more important due to a growing interest in designing and optimizing process using complex mathematical models. Especially, the sequential modular process simulator has

many advantages due to its features that; 1) process unit models are pre-coded and fixed as subroutines, 2) a library is made available to the user, 3) stream structure is fixed such as flow rate, temperature, and pressure, 4) solution procedures are embedded in subroutines with unit model equations, 5) directionality of inputs and results of unit model calculations is fixed to solve for the outputs with given inputs, and 6) sequential solution procedure of units from feed to product streams is conducted. According to above, the sequential modular approach process simulator has strengths to use easily for process analysis and solve the process model robustly.

On the other hand, there are several limitations to use commercial sequential modular simulators for the optimization-based process design. The most commercial sequential modular simulators do not allow to access to the original code, and it is not available to get any derivative information [18]. In addition, it often shows inconsistent errors in simulation results due to the tolerance to solve recycle streams iteratively [19]. In this respect, it would be more proper to use equation-oriented simulators in order to find optimal design because the solution to equation-oriented models has been demonstrated as effective in solving optimization, problems [20]. However, equation-oriented simulators still have a disadvantage that the general purpose nonlinear equation solvers are not as robust and reliable as the sequential modular approach in case of steady state

simulation [20, 21].

In this thesis, the general-purposed sequential modular simulator is used to make the modeling and analysis of steady state simulation of chemical processes much easier and convenient. And its limitations, mentioned above, will be overcome by means of new solution procedure integrated with simulator.

1.3 Scope of Thesis

This thesis aims to propose the sustainable design framework using commercial process simulator, with an emphasis on the quantification of sustainability and improvement of calculation time to determine optimal design variables. A sustainable design is in close association with innovation considering new design variables with process specifications and new methods for process analysis. It should be conducted during a certain design stage when the freedom of design is sufficient to make significant contributions to reduce investments and operational costs and implementation of risk reduction. Therefore, the preliminary design stage (the dotted rectangular box in Figure 1-2) is the most effective area for making a sustainable design because it allows diverse modifications of a design with respect to innovative sustainability intensification

as well as improvement of economical efficiency.

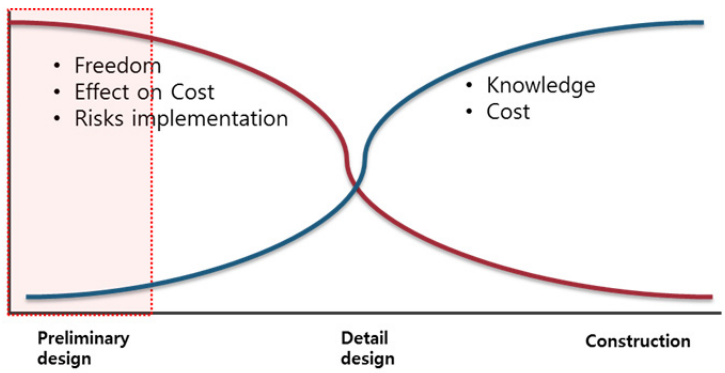

Figure 1-2 Design freedom, impact, knowledge and cost versus project time [22]

The use of a commercial process simulator is essential for the design and optimization of chemical processes during the preliminary design stage, but the rational solution procedure should be proposed because the commercial simulator has drawbacks to; 1) determine optimal design variables with the consideration of sustainability and 2) extend the boundaries of analysis conducted by the traditional material and energy balance. Thus, the statistical black-box optimization strategy is introduced and its performance is verified in Chapter 2.

The optimization methodology with commercial simulator must be enabled to determine the optimal solution of many design variables simultaneously because the degree of freedom at the preliminary stage is much higher than the one at the latter stage as shown in Figure 1-2. However, the more design variables to be determined by the statistical black-box optimization strategy exist, the more time is needed to solve the problem. Therefore, the solution framework, integrating sustainable performance evaluation with economic analysis using commercial simulator, is proposed in order to offer more rational strategy in terms of time complexity in Chapter 3.

The applications to the process design problem using above solution procedure is presented in Chapter 4 and 5. The first application in Chapter 4 is to design optimal process of offshore oil and gas production facilities with the consideration of environmental aspect. The second one in Chapter 5 is to design optimal dual mixed refrigerant LNG process with respect to safety aspect. These two applications are to identify sustainability as well as economic performance, and it will demonstrate convincingly that the proposed procedure is effective and efficient for sustainable process design. Lastly the thesis will be summarized and concluded in Chapter 6.

Chapter 2. Covariance Matrix Adaptation Evolution Strategy

Sequential modular simulator has a limitation in optimization. It is not available to obtain gradients to apply deterministic optimization methods [18], and if possible, it is difficult to apply deterministic optimization strategies because the simulation results slightly vary with repeated executions due to the tolerance for loop convergence [19]. It means that the objective function of design problem has many local optima owing to inconsistent error of simulation results. Therefore, a derivative-free direct search algorithm, which regards a process simulator as a black-box, is suitable for optimizing a complex process model.

2.1 Black-box Optimization

The engineers in various disciplines have encountered solving optimization problems originated from complex systems as shown in Figure 2-1. When the design problems can be formulated with differentiable objective, it is available to apply efficient solution methods such as Newton-type methods, interior point methods and SQP method. However, it is often hard to formulate mathematical

models explicitly as a differentiable form, especially in highly complicated systems, and if possible, it would be difficult to overcome local optima and determination of discrete decision variables of the models.

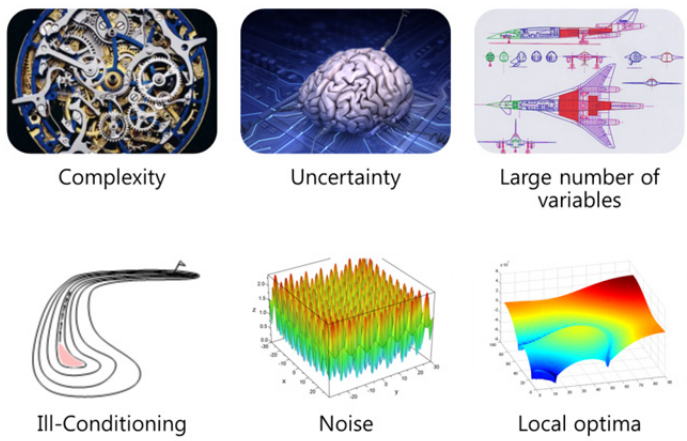

Figure 2-1 Difficulties to design and optimization in engineering disciplines

Numerous statistical approaches for the derivative free optimization have been introduced to a black-box optimization applied to a function $f(x): \mathbb{R}^n \to \mathbb{R}$ for which the analytic form is not known or the properties of f are unknown a priori (independent of experience). The genetic algorithm (GA) and particle swarm optimization (PSO) are famous computation technique which searches

near-optimal solutions in a practical time, instead of finding exact optimal solutions in very long time [23]. The GA is based on the evolutionary mechanisms and mimics the process of natural selection consisting of mutation, crossover, inversion, and selection operators. The PSO imitates the swarm behavior of fish and bird in which each particle shares certain information (e.g. position and velocity) with other particle, and decides the next movement by the information. These are point-to-point approaches instead of population based approaches.

2.2 Covariance Matrix Adaptation Evolution Strategy

The CMA-ES is a direct search method for parameter optimization of non-linear and non-convex multimodal problems in the real-valued domain, and a major branch of evolutionary algorithms. It has the excellent capability of dealing with discontinuous and noisy functions which have local optima because it is based on the Gaussian random mutations [24]. CMA-ES takes account of quadratic information similar to quasi-Newton methods, since the covariance matrix updated in the CMA-ES is regarded as the inverse Hessian matrix on convex-quadratic functions [25].

The main reason why the CMA-ES is selected for this thesis is its capability of finding a higher accuracy solution with fewer function evaluations compared with 31 algorithms from other black-box optimization methods [26]. Moreover, it has much fewer settings required by the user than other statistical black-box optimization methods [27]. In contrast to binary encoded GA, CMA-ES makes the best use of knowledge about the real-valued domain since it operates on a phenotypic level [28].

The CMA-ES is a population based approach which is similar to a typical local search, since it conducts neighborhood search of the current point and moves to the next point using the evaluation of object function. Outline of general population based approach for black-box optimization is written as shown in Table 2-1.

Table 2-1 Statistical black-box search template

Step1)	Generate sets of λ sampling points $x_1, \cdots x_\lambda \in \mathbb{R}^n$ so that the sampling points follow the normal distribution $Pr(x)$ with given distribution parameters θ.
Step2)	Evaluate $x_1, \cdots x_\lambda$ on the objective function f.
Step3)	Update the distribution parameters θ according to distribution parameter updating procedure, $F_\theta\big(\theta, x_1, \cdots, x_\lambda, f(x_1), \cdots, f(x_\lambda)\big)$.

The performance of this procedure depends on the definition of distribution Pr and distribution parameter updating procedure F_θ, and the update of θ is more crucial element because the choice of distribution Pr and population λ is often decided before the optimization [29]. In most evolution strategy, the distribution is implicitly defined via operators on a population, selection, recombination and mutation, and parameters θ are composed of mean vector, step-size (standard deviation) and covariance matrix of the normal distribution.

$(\mu/\mu_w, \lambda)$-CMA-ES, used in this study, generates sets of sampling points to

the normal distribution, and searches for the optimal solution by updating the multivariate-mean vector, step-size and multivariate-covariance matrix [30]. $(\mu/\mu_w, \lambda)$-type of CMA-ES selects μ points of parents from the sampled λ points of offsprings only and updates the mean of the next generation with a weighted recombination of μ points (μ_w). The scheme of CMA-ES is presented in Table 2-2.

Table 2-2 Scheme of CMA-ES

Step 0. Set initial parameters) Set parameters to their default values
Step 1. Initialization) Set evolution paths equal to zero Set covariance matrix $\mathbf{C}^{(0)} = \mathbf{I}$, and number of generation $\mathrm{g} = 0$ Input distribution mean $m^{(0)} \in \mathbb{R}^n$ and step size $\sigma^{(0)} \in \mathbb{R}_+$
Step 2. Termination criterion) If termination criterion met, then stop
Step 3. New population sampling) $x_i^{(\mathrm{g}+1)} \sim \mathcal{N}\left(m^{(\mathrm{g})}, \left(\sigma^{(\mathrm{g})}\right)^2 \mathbf{C}^{(\mathrm{g})}\right)$ for $i = 1, \cdots, \lambda$
Step 4. Recombination and selection) Recombination of sample point in order of best individual
Step 5. Update parameters) Update weighted mean value $m^{(g+1)}$ of μ selected offspring Update covariance matrix $\mathbf{C}^{(g+1)}$ and step-size $\sigma^{(g+1)}$ Go to **Step 2**

2.2.1 Historical Review of CMA-ES

The covariance matrix adaptation is introduced into the $(1,\lambda)$-ES by Nikolaus Hansen in 1996 [31]. It extended with the weighted recombination and so-called 'multi-membered' (μ,λ)-ES in 2001 [27] and 'rank-μ-update' of the covariance matrix which improves the efficiency of the CMA to large population sizes and reduces the time complexity (i.e. the number of generations to adapt the complete matrix roughly from $10n^2$ to $20n$) [30]. Finally, for the large population sizes, the weighted non-uniform recombination and improvement of parameter setting for the step-size adaptation was introduced in 2004 [24].

2.2.2 Sampling Points Generation

The searching points with λ population size at the (g+1)-th generation are sampled so that they follow the normal distribution at the (g)-th generation.

$$x_i^{(g+1)} \sim N\left(m^{(g)}, \left(\sigma^{(g)}\right)^2 \mathbf{C}^{(g)}\right) \qquad \text{for } i = 1,\cdots,\lambda$$
$$\text{where } x_i, m \in \mathbb{R}^n,\ \sigma \in \mathbb{R}_+,\ \mathbf{C} \in \mathbb{R}^{n\times n} \tag{1}$$

The symbol '~' denotes the same distribution on the left and right side. The mean vector m represents the favorite solution, the step-size σ controls the

step length, and the covariance matrix $\mathbf{C}$ determines the shape of the distribution ellipsoid.

2.2.3 Selection and Recombination

The new mean vector of the search distribution is updated by a weighted average of μ selected points (offspring) from the samples $x_1^{(g+1)}, \cdots, x_\lambda^{(g+1)}$.

$$m^{(g+1)} = \sum_{i=1}^{\mu} w_i x_{i:\lambda}^{(g+1)} = m^{(g)} + \sum_{i=1}^{\mu} w_i (x_{i:\lambda}^{(g+1)} - m^{(g)})$$
$$\text{where, } \sum_{i=1}^{\mu} w_i = 1, \quad w_1 \geq w_2 \geq \cdots \geq w_\mu > 0 \tag{2}$$

The index '$i:\lambda$' denotes the i-th ranked individual where $f(x_{1:\lambda}^{(g+1)}) \leq \cdots \leq f(x_{\lambda:\lambda}^{(g+1)})$ and f is the objective function to be minimized. In this thesis, the half-selection method is imposed after recombination (i.e. $\mu = 1/2\,\lambda$) because, on a linear or sphere function in expectation, the better half of the new candidate solutions improve over mean value.

2.2.4 Covariance matrix updating

The adaptation of weighted covariance matrix exploits the so-called 'rank-μ-update' and 'rank-one-update'. The rank-μ-update estimates the distribution of selected steps of favorite solutions as shown in Eq. (3) and Figure 2-2.

$$\text{rank-}\mu\text{-update} : \sum_{i=1}^{\mu} w_i \left(\frac{x_i^{(g+1)} - m^{(g)}}{\sigma^{(g)}} \right) \left(\frac{x_i^{(g+1)} - m^{(g)}}{\sigma^{(g)}} \right)^T \tag{3}$$

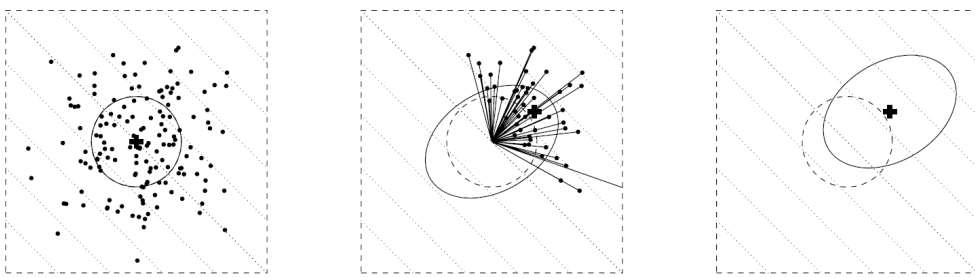

Figure 2-2 Rank-μ-update for covariance adaptation [32]

Figure 2-2 presents the schematic depiction of sampling (left), estimation (center), and new distribution covariance matrix (right), respectively. The rank-μ-update, considering the variation of selected individuals (solid straight lines in the center of Figure 2-2), contributes to improvement of learning rate for large population, and the sum of outer products in Eq. (3) is of rank $\min(\mu, n) = \mu$ when the selected offspring size μ is greater than the number of variables n in optimization.

The rank-one-update utilizes the evolution path which means the cumulative information of the mean trajectory in each generation, where $c_c < 1$ and constant Π selected as $Z_c^{(g+1)} \sim \mathcal{N}(0, \mathbf{C})$, as shown in Eq. (4) and Figure 2-3. It exploits the best solution individual of parent and its outer product is of rank one.

rank-one-update (evolution path) :

$$Z_c^{(g+1)} = (1 - c_c) Z_c^{(g)} + \Pi \frac{m^{(g+1)} - m^{(g)}}{\sigma^{(g)}} \tag{4}$$

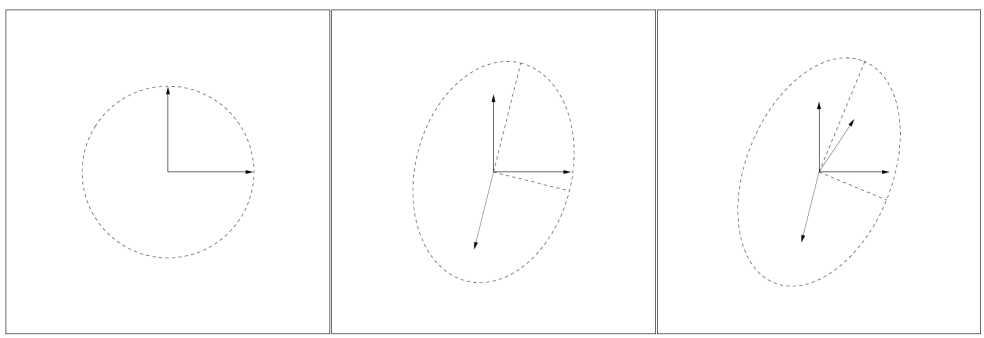

Figure 2-3 Rank-one-update for covariance adaptation [33]

By using rank-one-update correlation, it is available to update covariance matrix reliably if population size λ is small [23]. The final weighted covariance adaptation with the weighted coefficient w_i and weighted average m, combining rank-μ-update and rank-one-update, is shown in Eq. (5);

$$C^{(g+1)} = (1-\nu)C^{(g)} + \nu\left(1-\frac{1}{\xi}\right)\sum_{i=1}^{\mu} w_i \left(\frac{x_i^{(g+1)} - m^{(g)}}{\sigma^{(g)}}\right)\left(\frac{x_i^{(g+1)} - m^{(g)}}{\sigma^{(g)}}\right)^T + \frac{\nu}{\xi} Z_c^{(g+1)} Z_c^{(g+1)^T} \quad (5)$$

, where learning ratio $0 < \nu \leq 1$, choosing ratio ξ, and evolution path Z_c.

2.2.5 Step-size updating

The step-size σ updating is a path length control procedure. The correlation of mean trajectory by Z_σ, having similar structure to covariance evolution path, is described in Eq. (6) where $c_\sigma < 1$ and a constant η selected as $Z_\sigma^{(g+1)} \sim \mathcal{N}(0, \mathbf{C})$. By using step-size evolution path, it is available to update formula of $\sigma^{(g)}$ as shown in Eq. (7).

Step-size evolution path :

$$Z_\sigma^{(g+1)} = (1-c_\sigma)Z_\sigma^{(g)} + \eta\left(\mathbf{C}^{(g)}\right)^{-1/2} \frac{m^{(g+1)} - m^{(g)}}{\sigma^{(g)}} \quad (6)$$

Step-size control :

$$\sigma^{(g+1)} = \sigma^{(g)} \times \exp\left(c_\sigma\left(\frac{\|P_\sigma\|}{E\|N(0,I)\|} - 1\right)\right) \quad (7)$$

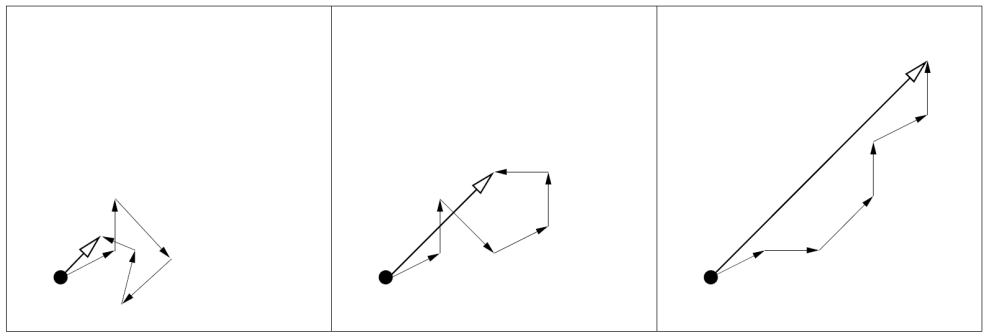

Figure 2-4 Schematic depiction of three evolution paths in the search space [29]

As shown in Eq. (6-7) and the right side of Figure 2-4, the larger mean trajectory $m^{(g+1)} - m^{(g)}$ and evolution path $Z_\sigma^{(g+1)}$ are, the larger $\sigma^{(g+1)}$ is. On the contrary, as shown in Eq. (6-7) and the left side of Figure 2-4, the smaller mean trajectory $m^{(g+1)} - m^{(g)}$ and evolution path $Z_\sigma^{(g+1)}$ are, the smaller $\sigma^{(g+1)}$ is. Therefore, step-size is controlled by mean trajectory correlation.

2.3 CMA-ES Benchmarking

2.3.1 Benchmarking Strategy

The CMA-ES has several advantages in combining with a black-box model with complex structure. It is reported that CMA-ES has the capability of finding a higher accuracy solution with fewer evaluations compared with other meta-heuristic methods such as the GA or PSO [26, 34].

In this thesis, CMA-ES is compared with PSO, real-coded GA, and simple GA to verify the performance of CMA-ES with respect to reliability and time complexity. First, the five test functions, shown in Figure 2-5~9, are chosen from the twenty four noiseless functions presented by Finck, et al. [35] for this experiment.

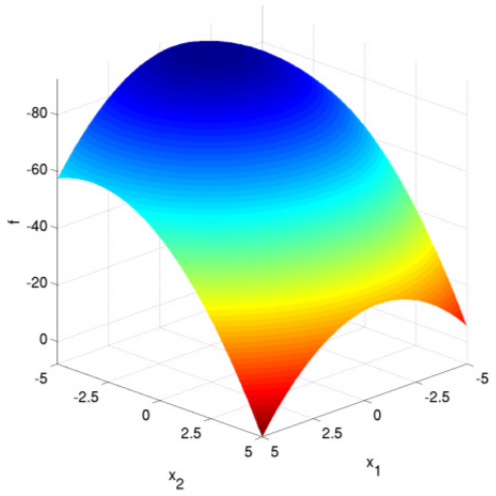

Figure 2-5 Sphere test function among the separable functions [35]

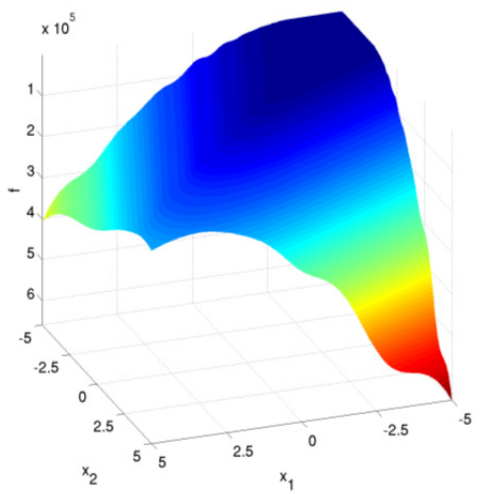

Figure 2-6 Attractive sector test function among the functions with low or moderate conditioning [35]

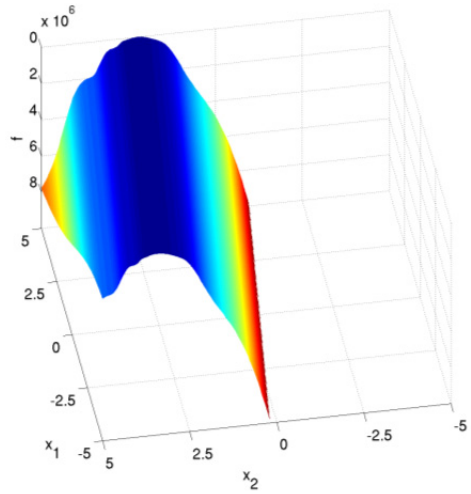

Figure 2-7 Ellipsoidal test function among the functions with high conditioning and unimodal [35]

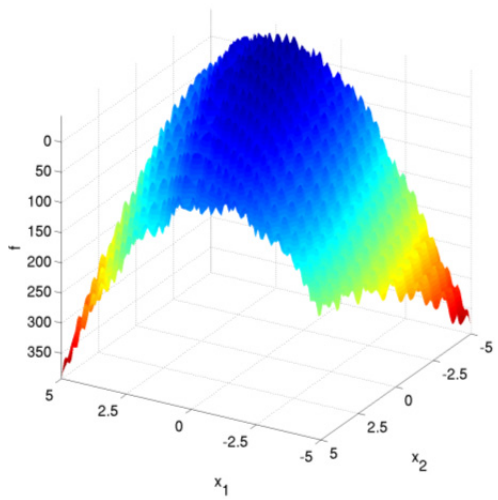

Figure 2-8 Rastrigin test function among the multimodal functions [35]

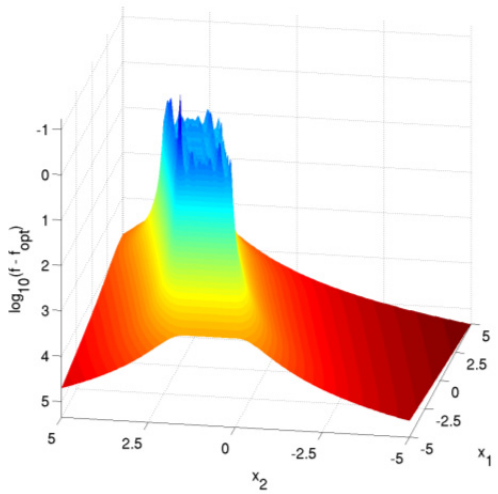

Figure 2-9 Schwefel test function among multimodal and weak global structure functions [35]

As shown in figures above, making a brief introduction, (a) the sphere function is presumably the most easy continuous domain search problem which is unimodal and highly symmetric (Figure 2-5), (b) the attractive sector function is a highly asymmetric function which is unimodal and has only one hypercone (Figure 2-6), (c) the ellipsoidal function is globally quadratic ill-conditioned function (Figure 2-7), (d) the Rastrigin function is a highly multimodal function which has a very regular and symmetric structure for the placement of the global optima (Figure 2-8), and (e) the Schewefel function is a multimodal function

with the weak global structure, and it is essential to identify the effect of penalization for constrained optimization problem (Figure 2-9). Ill-conditioning is a challenge in optimization, besides multimodality [36]. In case of convex quadratic functions, the condition number corresponds to the square root of the ratio between the longest and shortest axis of the ellipsoid due to the fact that contour lines associated to a convex quadratic function are ellipsoids. Similarly, expanding more general functions, conditioning has relevance to the square of the ratio between the largest and smallest of a contour line. The test function contains ill-conditioned functions with a typical conditioning of 10^6 [35].

The comparison study is conducted by the methodology proposed by Hansen, et al. [37]. The optimization algorithm under consideration is run on the test functions to be minimized, and the target precision is a kind of tolerance between known optimal value and evaluated function value. The setting to quantify and compare performance of numerical optimization algorithms is presented in Table 2-3. The target function value for all cases is $f_{optimal} + 10^{-3}$. For all cases of five test functions, it is not hard to reach a value of $f_{optimal} + 10^{0}$ but it often falls into local optima. It cannot assure that the target function value of $f_{optimal} + 10^{-3}$ is intrinsically 'very good' but it is regarded as reasonable precision through the experiment results in case of five test functions.

Table 2-3 Setting for comparison experiment

Precision	$\Delta f = f_{optimal} - f_{evaluation} = 10^{-3}$
Number of trials	15
Function dimension	2-D and 10-D
Searching space	$[-5, 5]^D$ where $D = 2, 10$
Experimental algorithms	CMA-ES, PSO, Real-code GA, Simple GA
Max. number of evaluation	200,000 for 2-D and 1,000,000 for 10-D

The main comparison approach for making measurements from experiments is a fixed-target scenario which fixes a target function value (tolerance) and measures the number of function evaluations needed to reach this target function value. In addition, the fixed-cost scenario which is close to what is required for real world problems is used to restrict meaningless function evaluation. Nevertheless, the fixed-target approach, used for this comparison experiment, is worthwhile to quantify and interpret the experiment data due to the fact that it measures a time complexity need to reach a target function value and makes a conclusions to the questions: 'How many times faster than other algorithms?'.

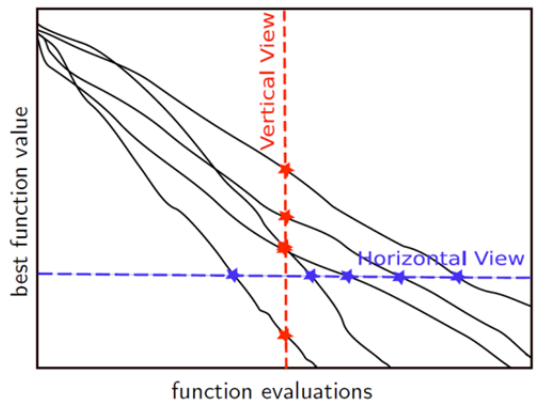

Figure 2-10 Fixed-cost (vertical view) and fixed-target (horizontal view) approach for comparison experiment

The number of trials is to identify the reliability of each algorithm. All the experiment repeats the same execution 15 times and it is summed up how many times it fails to find the optimal solution.

2.3.2 Benchmarking Results

Figure 2-11~15 present the comparison results of the five test functions. The purple bar means the variation above average function evaluation and the green bar means the variation below average function evaluation. The solid straight line presents the distribution of the number of function evaluation including maximum and minimum value achieved by fifteen times executions repeatedly. The black triangular block shows the number of failures during fifteen times executions, and the low failure number implies that the algorithm is more reliable.

In all cases, the CMA-ES shows the results that: 1) it is a reliable algorithm due to not only the fact that there is no failure in all experiments but also the comparison results with PSO and two types of GA, and 2) it has the capability to find solution with higher accuracy than other algorithms. These features of CMA-ES prove its real worth as a global optimization algorithm when the dimension of variable is increased. It is the only algorithm to find solution fast and reliably to the ill-conditioning, multimodal, and weak global test functions.

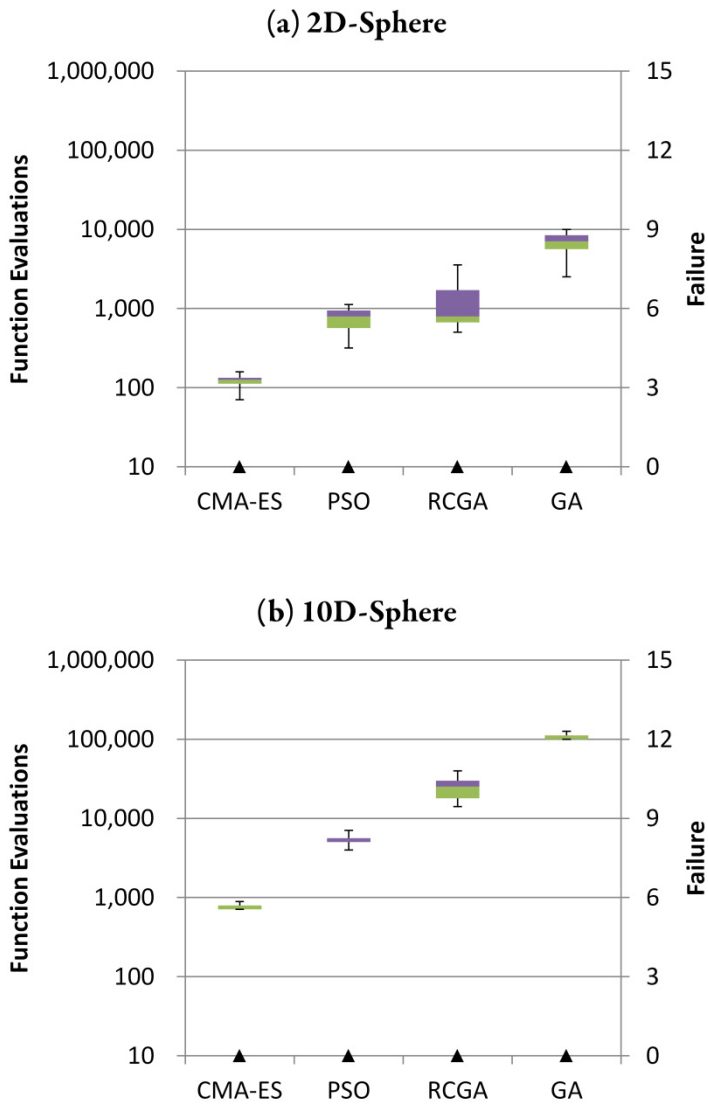

Figure 2-11 Comparison results of sphere function

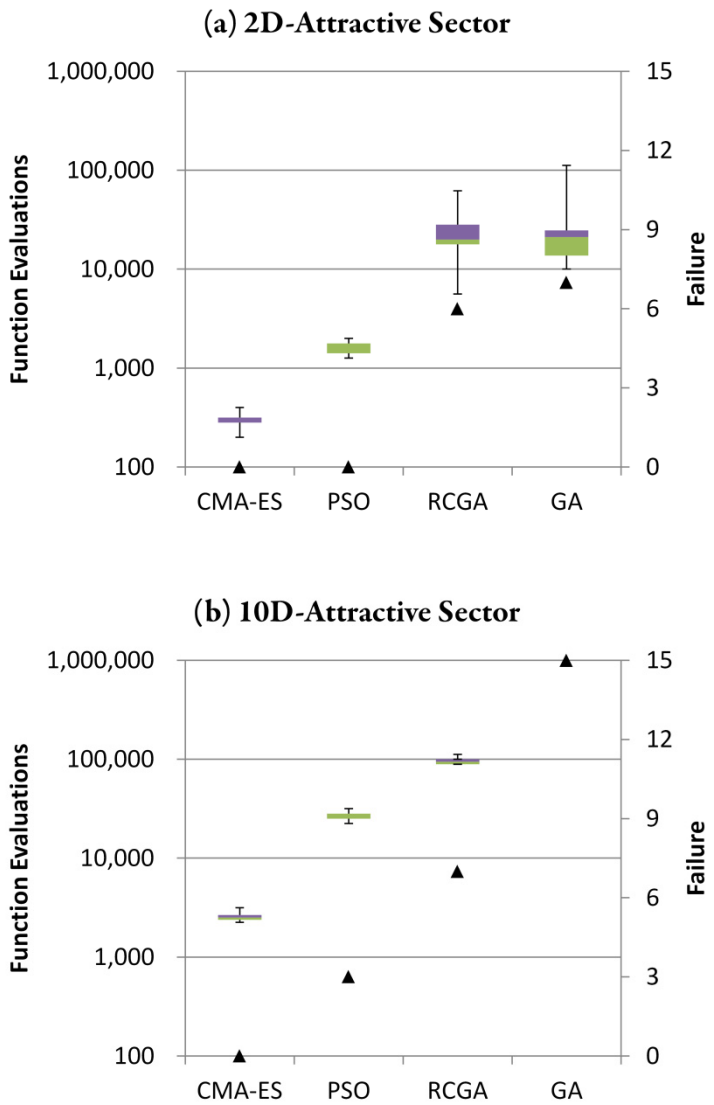

Figure 2-12 Comparison results of attractive sector function

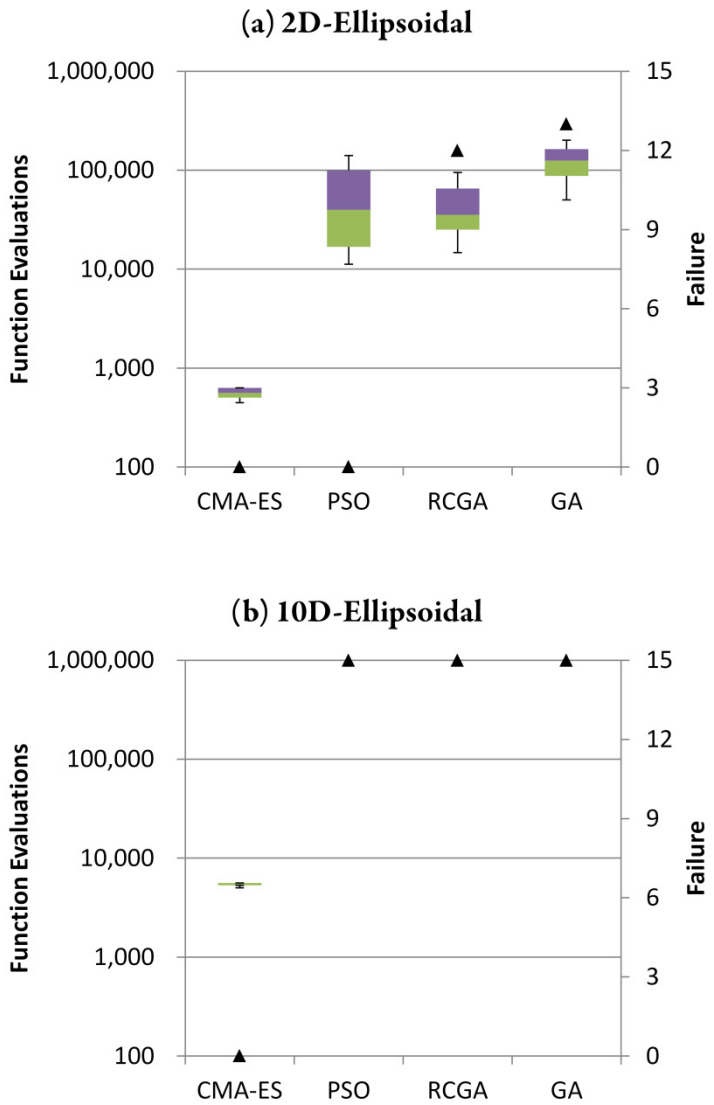

Figure 2-13 Comparison results of ellipsoidal function

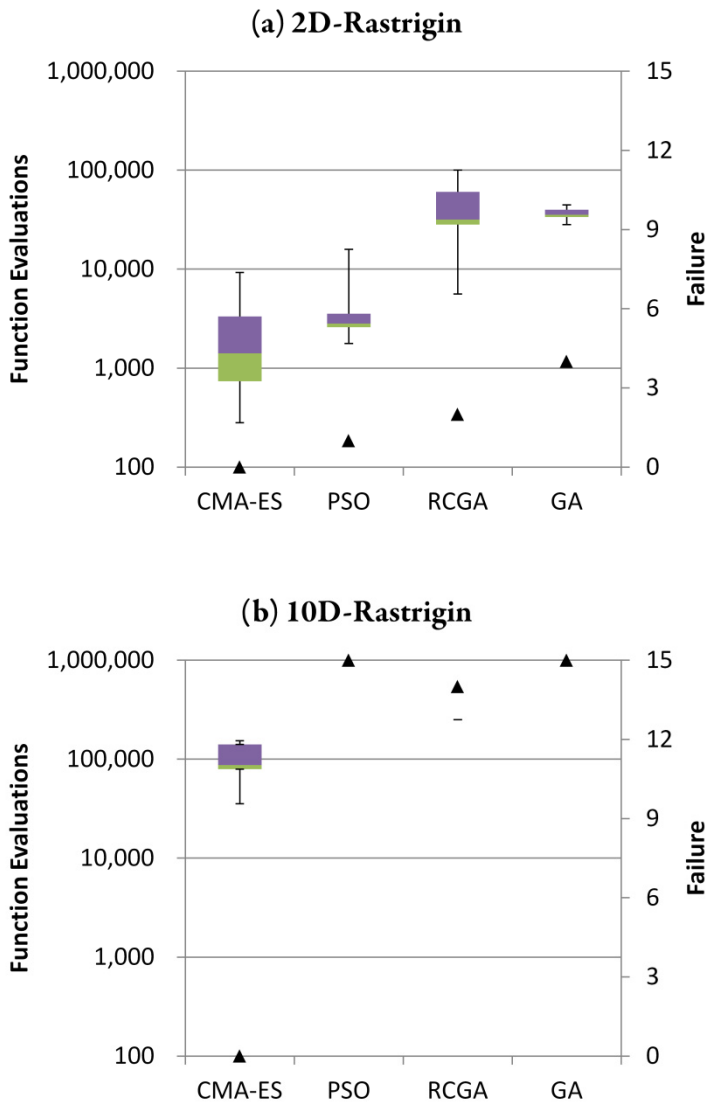

Figure 2-14 Comparison results of Rastrigin function

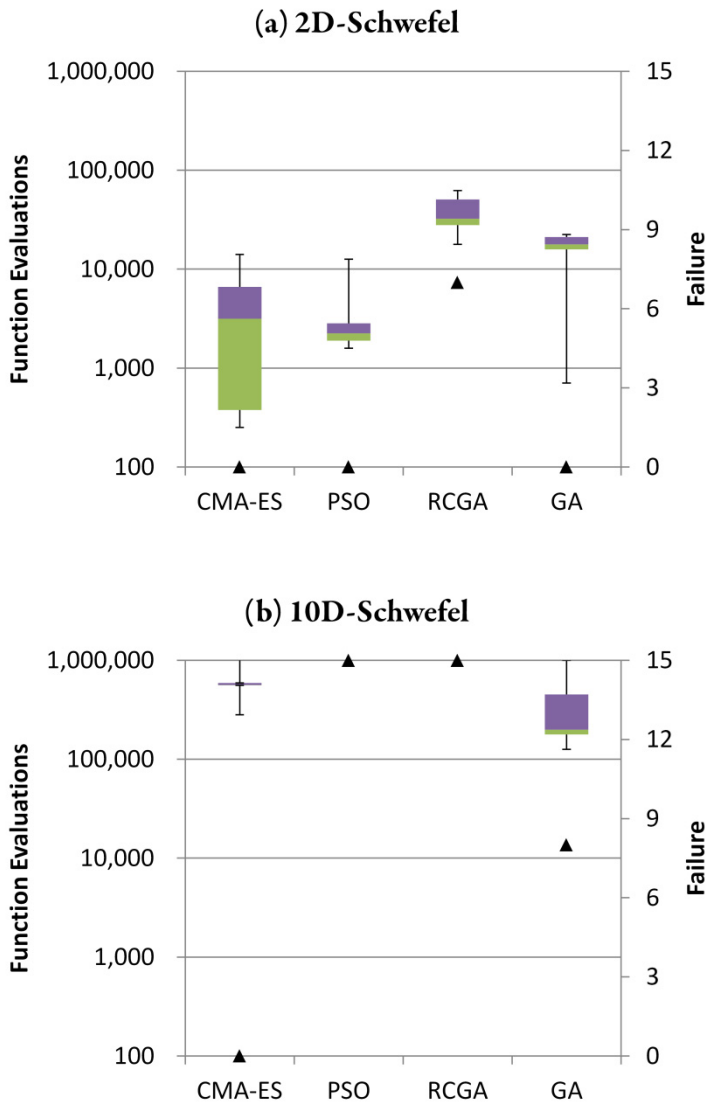

Figure 2-15 Comparison results of Schwefel function

2.4 CMA-ES for Constrained Problems

Similar to other statistical black-box optimization methods, CMA-ES originally is for unconstrained optimization problems [38]. It should be extended to solve constrained optimization problems by using the additional methods to handle the constraints such as penalizing infeasible individuals, rejection of infeasible individuals, repair of infeasible individuals, replacement of individuals by their repaired versions, separation of individuals and constraints, and so on [39]. Among these methods for handling constraints, two methods are adopted in this thesis: rejecting and penalizing infeasible individuals.

2.4.1 Rejecting Infeasible Individuals

The rejection method applies the so-called 'death penalty' returning back a high number of objective values without function evaluation so that it can prevent the algorithm from searching infeasible space.

This method is very helpful strategy to enlarge the searching domain without the simulation failure caused by physically unfeasible input specifications. Moreover, using rejection method, there is no need to waste much time to troubleshoot the consistency error incurred by unsuspected interaction between

processes and units. Therefore, rejection method is powerful to deal with various simulation failures and integrate the sustainability analysis of design and process simulation robustly.

2.4.2 Penalizing Infeasible Individuals

This method is the most favorable approach in the black-box optimization. The penalty method transforms the constrained optimization problem into the unconstrained configuration. Equation (8) represents the penalty method with k numbers of constraints and penalty function Φ which is equal to zero when $x \leq 0$, and increases when $x > 0$. In this thesis, the quadratic penalty function is used for the penalty method.

$$\begin{cases} \min f(x) \\ \text{s.t. } h_j(x) \leq d_j \quad {}^{\forall} j = 1, \cdots, k \end{cases} \\ \Rightarrow \min f(x) + \sum_{j=1}^{k} \left(\Phi\left(h_j(x) - d_j \right) \right) \tag{8}$$

Chapter 3. Sustainable Design Procedure

It is not easy to identify sustainability of chemical process because it is a broad concept related to economic, environment, safety, social aspects, and so on. During preliminary design stage, it is possible to make full use of ability of commercial simulator.

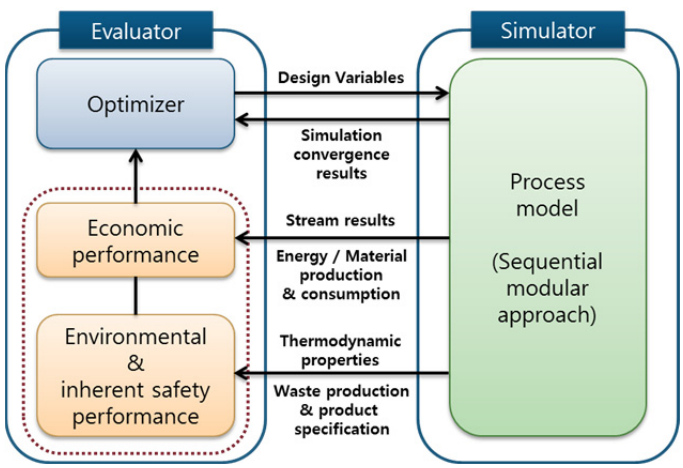

Figure 3-1 Integration for assessment of sustainability derived from simulation results

Especially, the environmental performance regarding the regulations of potential pollution and the inherent safety regarding toxic release, explosion and fire can be analyzed by thermodynamic properties of each stream and product. The economic performance is also computed by energy and material balance of overall process. Thus, the sustainable design procedure integrated with commercial simulator is competent to quantify and assess the sustainability during preliminary design stage as shown in Figure 3-1.

The proposed sustainable design procedure is presented in Figure 3-2. The overall solution procedure is an iterative process executing the nested loop. The sequential modular simulator is an inner loop to solve the process model, and optimization activity including sustainability and economic assessment is an outer loop. The two major disadvantages of this kind of procedure are that 1) it is very computationally expensive because the inner recycle loop must be converged for the each iteration on the outer recycle loop, and 2) the nested iterations tend to interact strongly and lead to severe convergence problems. .

In this thesis, reducing the time complexity can be achieved by fast converging algorithm, CMA-ES, described in Chapter 2, and the interactions between inner and outer loops is diminished by the rejection method shown in Chapter 2.4.1. The CMA-ES is an excellent algorithm to handle noisy results from simulation

tolerance and multidirectional process specification related to design variables. The rejection method is implemented in two locations: 1) to check the loop convergence of simulation results, and 2) to sort out the physically infeasible individuals from the sampling points generated by updated sampling distribution.

The modification of process model is to consider the discrete decision of cooling and heating media or pump and compression selection under given condition of individual. Initializing tearing stream makes the simulation results possible to reduce the accumulation of inconsistent tolerance errors.

In this thesis, the two kinds of sustainability performance are introduced: 1) environmental performance represented by GHG emission and waste disposal, and 2) inherent safety performance described by the quantitative risk analysis assuming worst case scenario.

The variable declarations for Aspen HYSYS automation with Matlab consist of two parts: 1) assessing the Aspen HYSYS objects of the input and output variables for optimization and 2) controlling Aspen HYSYS for the initialization of tear streams and turning the solver on and off supported by the COM/ActiveX interface of Matlab [40].

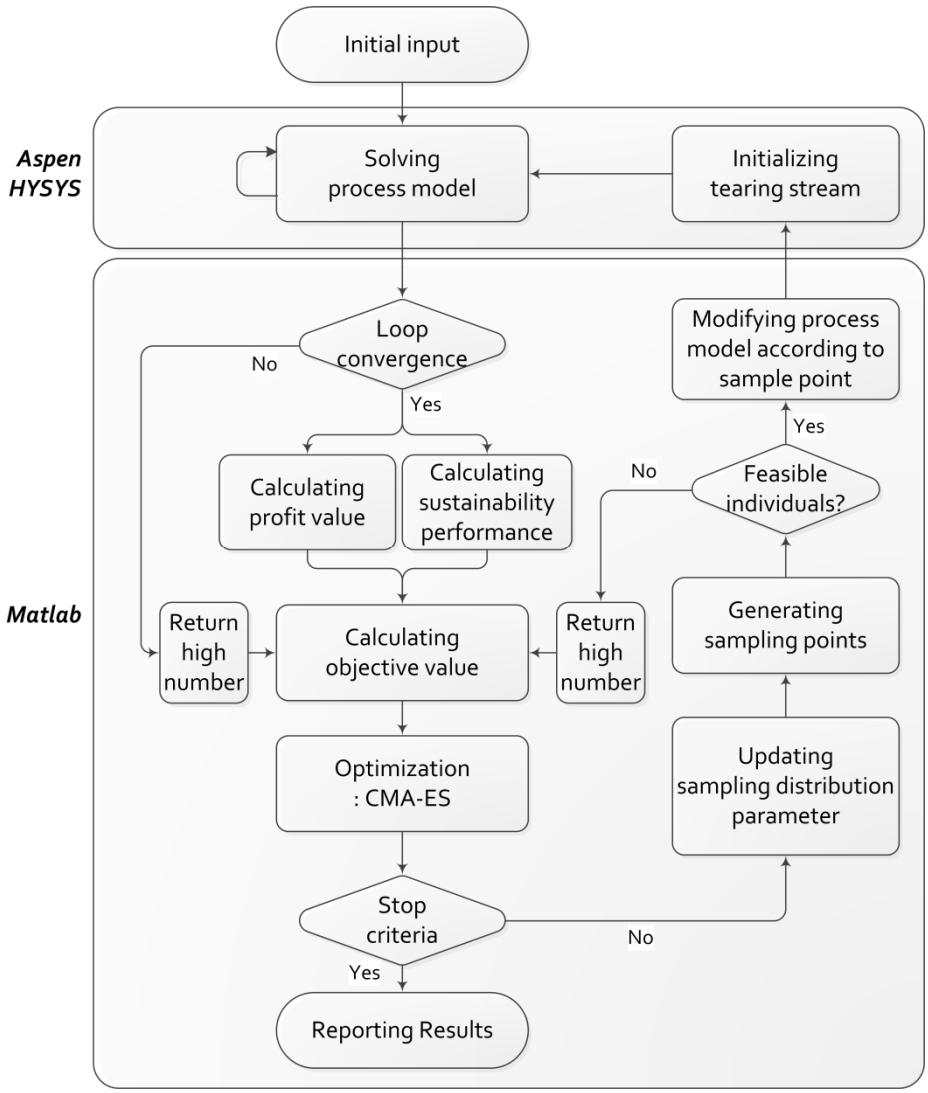

Figure 3-2 Proposed sustainable deign procedure

Chapter 4. Case Study I

4.1 Offshore Oil Production Process

Offshore oil production facilities are platforms that produce transportable oil and gas by pipelines and tankers. Offshore oil production facilities separate well fluids into three phases (oil, gas, and water) and remove impurities such as H_2O, N_2, CO_2, H_2S, etc. to make oil and gas that not only satisfy the specifications for storage and transportation but also for environmental regulations to prevent air and marine pollution. The process configuration and floating type of an offshore facility depend on the properties of the well fluids and geological features. Regardless of the region of installation, sequential three phase separators are used to process well fluids because of the limitation of space and utilities at the offshore platform [41]. Operating conditions are often determined by the characteristic features of the well fluid such as the composition of hydrocarbons and the amount of impurities.

From a process point of view, Abdel-Aal, et al. [42] describe the aim of oil production facilities in terms of separation performance: 1) separating the light components (C_1 and C_2) from oil, 2) maximizing the recovery of the intermediate components (C_3, C_4 and C_5) in the oil product, and 3) saving the

heavy components (C_{6+}) in the oil product. The light components contained in liquid oil flash to gas in the pipeline and storage tank. They cause economic loss during the transportation of liquid oil owing to its easy vaporization. On the other hand, intermediate components, which are the major substances that make up the crude oil, are liberated by undergoing a pressure drop through the separators. The most important design aspect of an offshore oil production facility is the performance of separating the light and intermediate components into gas and oil products to achieve the maximum oil recovery.

On the other side, the transportation and storage of crude oil are defined as a potential source of evaporation loss and flare gas which cause environmental contaminations. They should be restricted to prevent air pollution by volatile organic compound (VOC) [43, 44] and greenhouse gas emission by carbon dioxide and methane [45-47]. Because all kinds of evaporation losses and environmental influences cannot be estimated during the design of oil production facilities, Reid vapor pressure (RVP) is frequently used to consider the volatility and potential loss of crude oil as an indication of environmental pollutions. The RVP is defined as the absolute pressure exerted by oil or light hydrocarbons at 37.8 °C and it is intended for the thermodynamic stability of the crude oil under storage and transportation conditions [42, 45, 48]. Thus, the RVP is a key specification to design the oil production facilities as an

environmental consideration.

Figure 4-1 shows a pressure-temperature curve of hydrocarbon mixture utilized as a well feed in this study, and it is calculated by Aspen Properties. The reservoir is initially oversaturated, and the gas phase forms when the reservoir passes through the wellbore [49]. Separation conditions lie within the two-phase region. To achieve the process aim for a desired separation, adjusting pressure and temperature is the general strategies to separate liquid well fluid into the two-phases of oil and gas [49]. Choosing either pressures or temperatures of oil separators is not sufficient to determine the proper design variables for achieving an enhanced profit as well as satisfying environmental regulations.

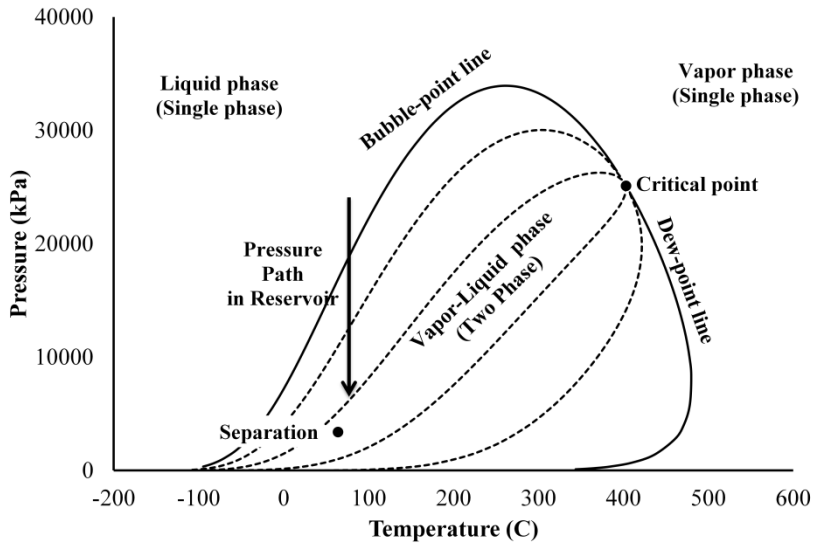

Figure 4-1 PT-phase curve of well feed

In designing sequential separators, maximum profit should be achieved by determining both the pressure and temperature of the separators to satisfy the environmental specification meeting its regulations or standards as in Eq. (9).

$$\begin{aligned} &Max.\ \ Profit = f(P_{sep},\ T_{sep}) \\ &\text{s.t. } h_{env}(P_{sep}, T_{sep}) \le d_{env} \end{aligned} \tag{9}$$

A multistage oil separation scheme at an offshore facility takes advantage of isenthalpic throttling in the valve leading to phase transformation. Furthermore, it does not require additional energy sources, which are often limited at an

offshore platform. As the well fluid is separated into three phases, the process should be divided into three functional sections; oil, gas and waste water treating trains. Whereas a model integrating all sections of the oil production process, can provide a comprehensive analysis of design and operations economics, the model often involves a large number of design variables and complex model structure. This makes it difficult to determine optimal values for design variables. For instance, additional condensation and separation utilities treating the gas stream give rise to increasing number of design variables and obscuring complex interactions among the units. Therefore, for the purpose of simplifying the model from an economic perspective, it might be practicable to consider only the performance of the oil treating train associated with the most valuable product in the process. This could be the reason why previous studies have focused on the design of multistage oil separation with the operation pressure of separators as a single optimization variable based on the simplified model illustrated in Figure 4-2.

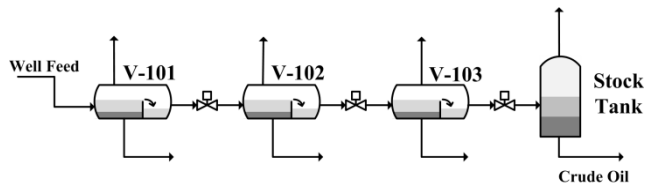

Figure 4-2 Simple scheme of multistage separation process [50]

Campbell [51] suggests a simple method for determining the pressure of a multistage separation process similar to a multi-compression system [52]. The intermediate stage pressure is determined by the total number of stages and the pressure of the first and last separators to minimize the compression cost. Whinery and Campbell [53] introduce an empirical correlation to determine the second-stage pressure for a 3-stage separation system. This correlation uses molecular weight and the composition of a well stream in addition to the first and last stage pressure. Mourad, et al. [46] report a graphical method to determine the intermediate stage pressure for minimizing compressor cost. This report employs commercial simulation software (Aspen HYSYS) and includes a condensate treating train though it only considers the compression cost.

Recently, gas-oil ratio (GOR), which means the rate of the volume of gas coming out of solution to the volume of oil at standard condition, has become a popular criterion to analyze the performance of a process although GOR has a

conflict with the relationship to oil recovery. Boyer and O'Connell [54] report an estimation of flash gas loss using both Aspen HYSYS and the sampling data of crude oil. Bahadori, et al. [55] report a hierarchical optimization method to minimize GOR sequentially with the stage order of the separators using Aspen HYSYS. Kylling [56] optimizes the profits in terms of oil sales and compression cost based on equation-based modeling and brute force optimization.

Although these studies attempted to find the optimal value for the operating pressure based on the operating cost or GOR, they did not consider environmental specifications for storage and transportation. An offshore oil production platform involves vapor pressure adjustment of the oil produced in order to comply with the RVP and the RVP specification varies from 69 to 83 kPa depending on local conditions [57]. However, it is difficult to show the relationship between design variables and the RVP of product oil explicitly though the oil production process model is simplified to consider the oil treating train only. Likewise, as the consideration of an offshore environment, a respectable amount of waste water is also significant factor to be considered during process design. Therefore, a novel design strategy is required that maximizes the economic potential and respects the environmental specifications considering all the oil, gas and waste water treating trains.

An offshore oil production platform also has a vapor condensation train to recycle the condensate back into crude oil to enhance the separation performance between light and intermediate hydrocarbons. The recycled streams may cause substantial increases in the consumption of compressor horse-powers and cooling water due to internally recycled materials. On the contrary, it can overcome the marginal performance of separation with the use of isenthalpic throttling alone so that the crude oil can have the lower RVP, namely eco-friendly product. In this case, the condenser temperature becomes an important design variable to generate and recycle an appropriate amount of condensate.

A multistage separation process has typically 2 to 4 stages in the oil production process, because for three or more stages, it is impossible to achieve a significant improvement with respect to GOR [57]. An oil production process with 2 or 3 stages is appropriate for 3.5~5.0 MPa of well feed pressure, and an additional stage is required in case more than 16,000 m^3 per day (100,000 barrels per day) of oil are produced [49]. It was also shown that 4-stage separation is usually optimal and enables a 2~12 % increase in oil recovery compared to a 3-stage separation process [55]. These guidelines take into account the crude oil recovery only. It is necessary to identify the improvement in performance more clearly in terms of the number of stages on the overall production rate and utility consumptions with the consideration of the RVP.

The object of this study is to find the maximum profit value calculated by the difference between product sales and operating costs for a multistage separation process. The Aspen HYSYS is used as the process simulator because of its capability for rigorous modeling and simulation of overall oil and gas production processes. The process model consists of an oil separation, gas condensation, waste water treatment and gas recompression train to reflect the interactions of all the equipment as well as represent a more realistic result considering profit value and environmental constraint. To clarify an effect of the existence of condensate recycling for the environmental consideration, the oil separation process without a condensation train is also employed to identify the maximum profit using the oil treating train only.

4.2 (Case 1) MSS without Condensate and Wastewater Recycle

The multistage separation process without condensation shown in Figure 4-3 additionally takes into account gas recompression based on the oil separation scheme shown in Figure 4-2. A number of studies have been conducted on the design of this process, and three aspects of this process are of interest: 1) maximum crude oil production [54, 55, 58], 2) minimum cost for gas recompression [46, 53] and 3) maximizing profit value [56]. In this study, the profit is calculated by not only oil sales and compression cost but also gas sales, cooling water cost, and waste water treating cost to provide an overall view of the total profit.

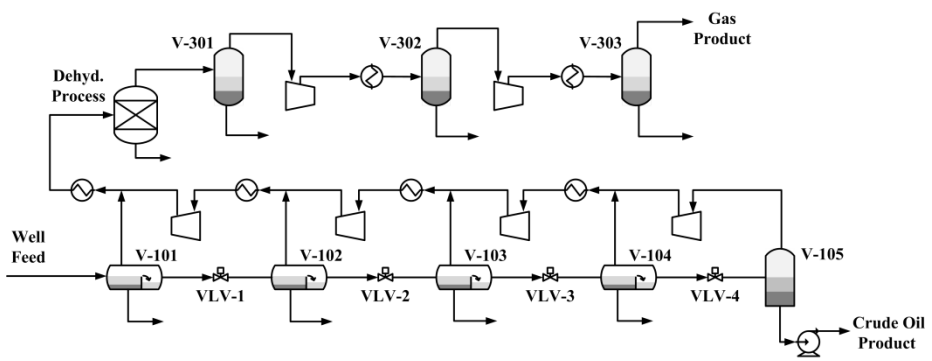

Figure 4-3 Four-stage MSS without condensation and wastewater recycle train [50]

In the case of four-stage MSS without condensation and waste water recycle shown in Figure 4-3, four pressure variables should be determined by the optimization. These design variables are the three intermediate stage pressures of the oil train (V-102, V-103 and V-104) and the intermediate stage pressure of the gas train (V-302). The first stage pressure of the oil train (V-101) is equal to the well feed condition, and the stock tank (V-105) pressure is specified as the atmospheric pressure.

Delivery pressure and gas temperature are the major concerns in the process design specifications for a natural gas pipeline are generally in the rage that temperature be less than 50 ˚C and pressure be greater than 5 MPa to avoid formation of condensate in the pipeline [42]. Multistage compression is a common solution to realize substantial savings in compressor energy consumption and to overcome the design limitation of a large pressure ratio [52, 59]. For a compressor operating in an efficient manner, the suction temperature should be lower to reduce the actual volume of the suction gas and to maintain the temperature within safe operating limits [60]. Thus, we assumed that the suction stream is cooled down to the dew point temperature to saturate gas and minimize the compression cost.

As mentioned earlier, multistage separation without condensation in Figure 4-

3 makes it difficult to adjust the RVP of the crude oil owing to the limitation of possible phase equilibrium induced by isenthalpic valve throttling only [50]. For this reason, the optimization results of this case neglect the RVP specification of the crude oil, and it is used for the comparison with Case 2 to identify the effect of condensate recycling and the change in the numbers of stages.

4.3 (Case 2) MSS with Condensate and Wastewater Recycle

A MSS with condensate recycling is shown in Figure 4-4. The condensate and wastewater recycling improves the crude oil recovery because of the intermediate hydrocarbons and wastewater back into the oil train. The notable change here is the use of a feed heater in the separation process. As the condensate cooled down to a lower temperature flows back into the oil train, it is possible to compensate for temperature loss by heating the well feed.

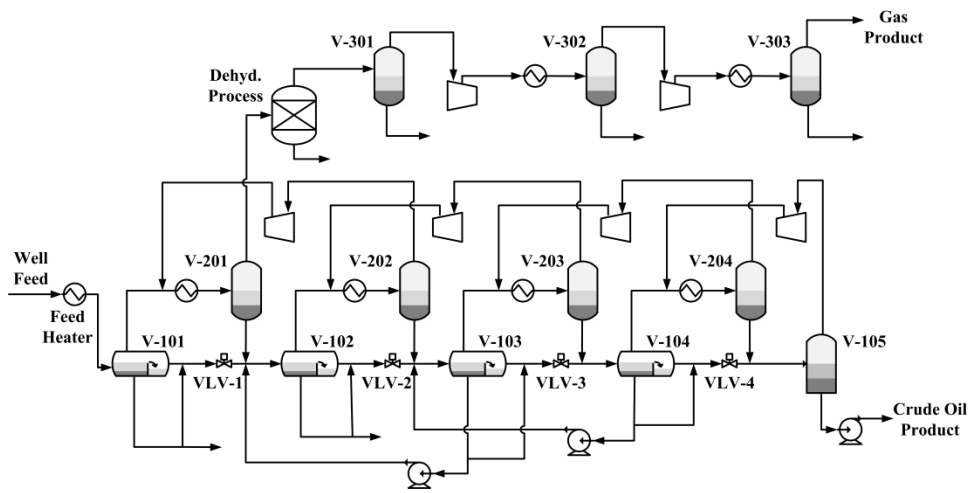

Figure 4-4 Four-stage MSS with condensation and wastewater recycle train

In this case, the temperature conditions of a feed heater, four condensers and four wastewater recycle ratios are added to the design variables for comparison

with Case 1. Thus, a total of thirteen design variables should be determined by the optimization. This process scheme has the capability of satisfying the environmental constraint referring to RVP of crude oil and minimizing wastewater production. Therefore, the optimization can deal with the profit value as well as the environmental considerations.

The condensate recycle is to treat gas stream and it improves the separation performance. On the contrary, the internal recycle flow causes operating cost to increase and the condensate cooling leads to decreased crude oil product temperature. Lowering temperature of crude oil product implies more liquid can be stored in the stock tank but it would be vaporized easily as the ambient temperature around the stock tanks increases during the daytime or summer season. In this respect, the feed heater is required to compensate for lowering temperature of crude oil product and it also contributes to reducing the internal flow rate utilized after the first oil separator (V-101) because more gas flow is generated in the first oil separator.

In Case 2 without consideration of RVP specification, it is more profitable to cool down the temperature of crude oil product as low as possible and minimize the use of feed heater because the crude oil product temperature is not considered. Hence, it does not need to consider the condensate recycling and

feed heating. However, in the case with RVP constraint (Case 2), as the RVP value is the property at the standard temperature, the separation performance between light and intermediate hydrocarbons becomes more important regardless of the crude oil temperature, and both the feed heating and condensate cooling need to be properly used. Thus, the condensate recycling with feed heating in Case 2 is considered as a way to satisfy RVP specification in the crude oil production process, and the results of Case 1 and 2 are not for identifying the recycling effects but for showing the differences in the optimal design with the consideration of RVP specification.

4.4 Problem Statement

The process model was developed with Aspen HYSYS. In all the cases, the well feed flowed into the process was assumed to be at 48.4 ˚C and 2,997 kPa, and the pressure of the first oil separator (V-101) was the same as the well feed condition. The composition of the well feed is presented in Table 4-1. The simulation of the multistage separation process contained pseudo-components which were equal to or heavier than C_{6+}. For the calculations of phase equilibrium, hydrocarbons heavier than C_7 were not critical components because the separation ratio of the light and intermediate hydrocarbons (from C_1 to C_5) from

the well feed is only crucial to lowering the vapor pressure specified as the RVP value [57]. For the same reason, Peng-Robinson equation-of-state model is suitable to predict the phase equilibrium and thermodynamic properties for the process simulation.

Table 4-1 Well feed composition

Component	Mole fraction (%)
H_2O	46.08
N_2	0.24
CO_2	1.76
C_1	25.47
C_2	3.50
C_3	3.11
i-C_4	0.59
n-C_4	1.74
i-C_5	0.77
n-C_5	0.85
C_6* (Sp.Gr.=0.6647, MW=86)	1.25
C_7* (Sp.Gr.=0.7432, MW=96)	1.72
C_8* (Sp.Gr.=0.7562, MW=107)	1.90
C_9* (Sp.Gr.=0.7676, MW=121)	1.48
C_{10-14}* (Sp.Gr.=0.8067, MW=158)	4.18
C_{15-20}* (Sp.Gr.=0.8496, MW=238)	2.58
C_{21-29}* (Sp.Gr.=0.8903, MW=336)	1.82
C_{30+}* (Sp.Gr.=0.9461, MW=535)	0.97

The stock tank for the crude oil was set at 117.2 kPa to provide a positive suction pressure for the last stage compressor [57]. The well feed flow rate was set at 17,006 kgmole/hr to produce about 16,000 m^3/day (100,000 bbl/day). Crude oil with 55.158 kPa of RVP was satisfactory, and the delivery condition of the gas product was at 48.9 °C and 18.857 MPa. It was assumed that the isentropic efficiency of the centrifugal compressor was 75%, and the pressure drop in the heater and cooler was 34.5 kPa. The input parameters and variables for the simulation are presented in Table 4-2. There are four design variables to determine in Case 1 and thirteen design variables in Case 2 regarding whether condensate and wastewater recycling is incorporated into the process.

Besides the input variables, the specification among the output values from the simulation is the RVP. The calculation of the crude oil RVP in Aspen HYSYS is performed by the 'ASTM D323' method which is the default HYSYS method because it is the most reliable for crude oil based on the wet basis so that the effect of water content in crude oil is considered [61]. It adjusts the pressure at the RVP reference temperature until the vapor to liquid ratio is 4:1 by volume.

Table 4-2 Input parameters and variables for simulation of MSS

	Initial value	**Case 1**	**Case 2**
Well feed composition	See Table 4-1	Fixed	Fixed
Well feed pressure (kPa)	2997.8	Fixed	Fixed
V-101 temperature (°C)	48.4	-	Variable
Pressure drop in VLV-1 (kPa)	1072.8	Variable	Variable
Pressure drop in VLV-2 (kPa)	1168.0	Variable	Variable
Pressure drop in VLV-3 (kPa)	459.2	Variable	Variable
V-105 pressure (kPa)	117.2	Fixed	Fixed
Temperature of V-201/202/203/204 (°C)	48.9	-	Variables
V-302 pressure (kPa)	9632.0	Variable	Variable
V-302 temperature (°C)	48.39	Fixed	Fixed
V-303 pressure (kPa)	18960.6	Fixed	Fixed
V-303 temperature (°C)	48.9	Fixed	Fixed
Wastewater recycle ratio in V-101/102/103/104	0	Fixed	Variables

4.5 Objective Function and Constraints

The objective of the optimization is profit maximization in all cases, as shown in Equation (10) and (11). The profit calculation is done by subtracting the operation costs of the steam, cooling water, electricity and wastewater treatment from the sales of the oil and gas. The constraint is the RVP value of the crude oil.

(Case1)

$$\max f_{profit}(x) = \left\{S_{Oil}(x) + S_{Gas}(x)\right\} - \left\{\sum U_{STM}(x) + \sum U_{CW}(x) + \sum U_{Elec}(x) + \sum U_{Waste}(x)\right\} \quad (10)$$

$$\text{s.t. } x_1 + x_2 + x_3 < 2880.6 \text{ kPa}$$

(Case2)

$$\max f_{profit}(x) = \left\{S_{Oil}(x) + S_{Gas}(x)\right\} - \left\{\sum U_{STM}(x) + \sum U_{CW}(x) + \sum U_{Elec}(x) + \sum U_{Waste}(x)\right\} \quad (11)$$

$$\text{s.t.} \begin{cases} RVP_{Oil}(x) \le 55.16 \text{ kPa} \\ BS \,\&\, W_{Oil} \le 0.2 \text{ vol\%} \\ x_2 + x_3 + x_4 < 2845.8 \text{ kPa} \\ x_5,\ x_6,\ x_7,\ x_8 < \text{cooler inlet temp.} \end{cases}$$

The design variables are summarized in Equation (12) and its bounds are presented in Table 4-3. The bounds of all design variables are scaled to [0, 10] by affine transformation [62]. The temperature of the first oil separator (V-101) and the pressure of the other oil separation trains (V-102, V-103 and V-104) are replaced by the changes in pressure and temperature so that the simulation can converge easily. The bounds of the design variables can cover all possible space to search for the global optimum. For instance, the pressure difference between the well feed and stock tank is 2880.6 kPa in Case 1, and it is possible to make the intermediate separator pressure negative regarding the search bounds of the oil separation pressure. Likewise, regarding the search bounds of the condenser temperature from V-201 to V-204, can lead to sample points of the condenser temperature for heating. Thus, the rejection method is adopted to avoid unrealistic simulation results caused by these infeasible individuals.

(Case 1) :

$$x = \left(\Delta P_{VLV-1},\ \Delta P_{VLV-2},\ \Delta P_{VLV-3}, P_{V-302} \right)$$

(Case 2) : (12)

$$x = \left(\Delta T_{V-101},\ \Delta P_{VLV-1},\ \Delta P_{VLV-2},\ \Delta P_{VLV-3} \right.$$
$$, T_{V-201}, \mathrm{T}_{V-202}, T_{V-203}, T_{V-204}$$
$$\left. , P_{V-302}, R_{V-101}, R_{V-102}, R_{V-103}, R_{V-104} \right)$$

Table 4-3 Upper and lower bounds of the design variables

Variable description	**Notation**	**Case 1**	**Case 2**
Temperature increase of well feed (°C)	ΔT_{V-101}	-	0 ~ 154.4
Pressure drop in VLV-1/2/3 (kPa)	$\Delta P_{VLV-1}, \Delta P_{VLV-2}, \Delta P_{VLV-3}$	69 ~ 2758	69 ~ 2758
Temperature of V-201/202/203/204 (°C)	$T_{V-201}, T_{V-202}, T_{V-203}, T_{V-204}$	-	21 ~ 94
Pressure of V-302 (kPa)	P_{V-302}	6205 ~ 15169	6205 ~ 15169
Recycle ratio of V-101/102/103/104	$R_{V-101}, R_{V-102}, R_{V-103}, R_{V-104}$	-	0~1

The prices of the products and utilities, presented in Table 4-4, are taken from the data provided by U.S. Energy Information Administration in January 2014, and the operation cost is calculated by the method in Seider, et al. [63]. It is assumed that the steam and cooling water are the media for heating and cooling for the simple representation of utility consumption, and three types of steam and two types of cooling water are introduced in order to cover a wide range of possible operating conditions and enable to choose the most optimal option.

This is a discrete decision-making problem which is able to be solved by the solution procedure proposed in Chapter 3. The wastewater cost is calculated by the tertiary treatment cost described by Ulrich and Vasudevan [64].

Table 4-4 Price of products and utility cost data

Items	**Price**	**Applicable temperature**
Gas product	$ 4.3 /MMBTU	18.96 MPa, 48.9 ˚C
Oil product	$ 93.0 /bbl	RVP = 55.16 kPa
LP Steam (445 kPa)	$ 6.60 / 1000 kg	≤ 130.9 ˚C
MP Steam (1135 kPa)	$ 10.50 / 1000 kg	≤ 169.0 ˚C
HP Steam (3200 kPa)	$ 14.50 / 1000 kg	≤ 221.6 ˚C
Cooling water	$ 0.020 /m^3	≥ 48.9 ˚C
Chilled water	$ 4.0 /GJ	≤ 48.9 ˚C, ≥ 21.1 ˚C
Electricity	$ 0.06 /kW-hr	-
Wastewater	Ulrich and Vasudevan [64]	

4.6 Solution Procedure

The solution procedure revised from Figure 3-2 is shown in Figure 4-5. For the initial inputs, the CMA-ES is operated with 100 and 300 populations in Case 1 and 2 respectively. And bounds of all design variables are scaled to [0, 10] by affine transformation [62]. This is very helpful in keeping the variables that have the same impact on the problem during the early generations so that the CMA-ES can find the global optimum without focusing on a certain space.

The sensitivities of stream parameters in the 'Recycle' block in Aspen HYSYS are lowered by one tenth of default value in order to reduce the effect of inconsistency error from the tolerance of recycle stream, and the simultaneous calculation mode is chosen with 200 numbers of maximum iterations in order to find the solution of totally six inter-connected recycles.

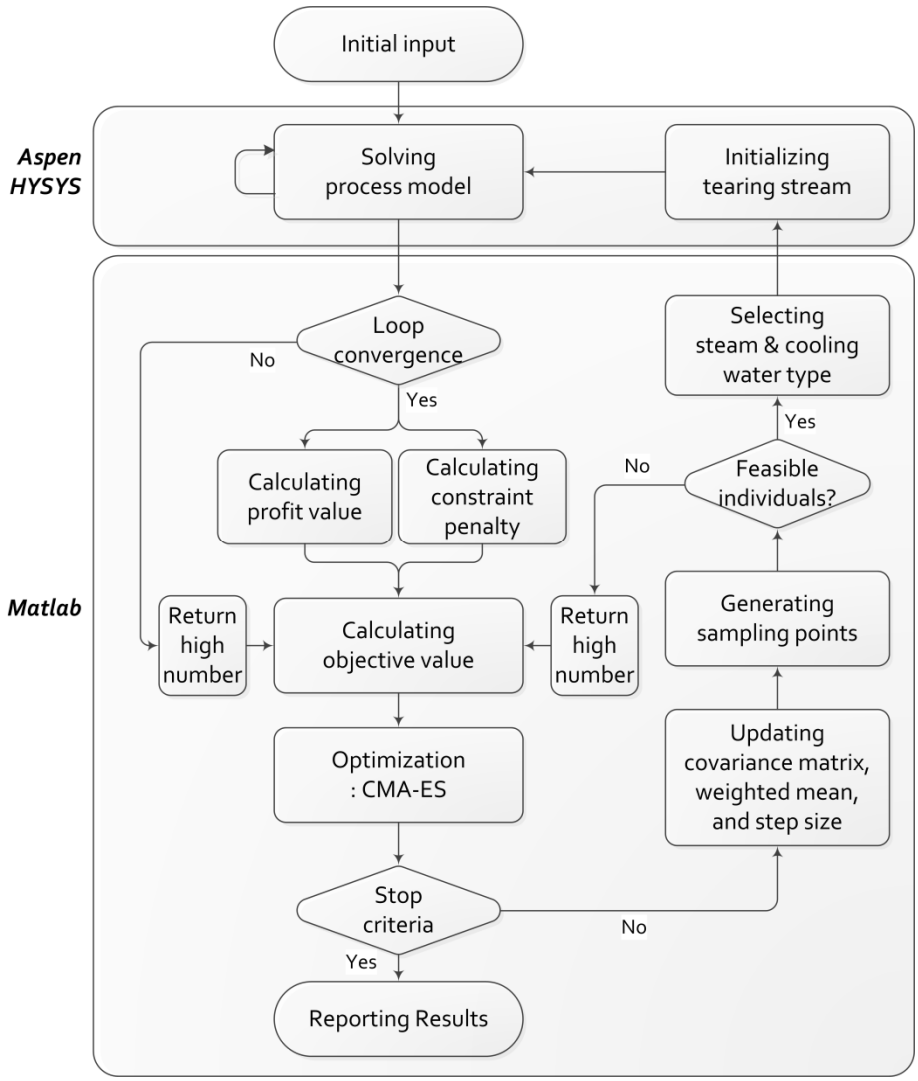

Figure 4-5 Solution procedure for optimizing oil and gas production process

The solution iteration in Figure 4-5 stops when the results of the CMA-ES satisfies the conditions presented in Table 4-5.

Table 4-5 Stopping criteria

Classification	**Stop criterion**
Variation of design variables	Less than 0.0001
Variation of objective function	Less than 0.01

4.7 Results and Discussion

The results of Case 1 don't take into consideration the RVP specification, as discussed in Chapter 4.2 and 4.3, because of the lack of capability to adjust the vapor pressure in the crude oil. It represents the maximum amount of light and intermediate hydrocarbons available in the atmospheric liquid oil. Because Case 1 employs isenthalpic throttling only, it is possible to identify the advantage of adopting temperature control by condensate recycling in Case 2.

The optimization results for maximizing profit are presented in Table 4-6. The variation in the profit for the two cases is $21,660/day. Presumably, it is a relatively small change because the crude oil produced contains about only 8 vol% of light and intermediate hydrocarbons, excepting of water contents. Nonetheless, as the capacity of offshore oil platforms continues to increase to more than 16,000 m^3/day (100,000 BPD) produced as well as the price of oil, it still represents distinctive improvement of the total profit.

The optimal operating conditions associated with the design variables are presented in Table 4-7. Compared with Case 1, the remarkable change in Case 2 is the increase in the operating pressure of the integrated process and about a 12.4 ˚C increase in the stock tank (V-105) temperature. The heating medium among the three types of steam (LP, MP, and HP steam) uses the LP steam at 445 kPa

only and the cooling medium used both the normal and chilled cooling water as needed.

Table 4-6 The result of profit and constraints

		Case 1	**Case 2**
Product sales ($/day)	Oil	9,725,452	9,778,598
	Gas	527,357	526,482
	Total	10,252,810	10,305,080
Utility cost ($/day)	Steam	0	16315
	Cooling water	513	12249
	Pumping	3288	3342
	Compressing	17725	20273
	Wastewater	4127	4084
	Total	25653	56263
Overall profit ($/day)		10,227,156	10,248,816
RVP of product oil (kPa)		72.81	55.16
BS&W in product oil (vol%)		0.0004	0.2

Table 4-7 Determined optimal operation conditions

	Case 1		**Case 2**	
	Temperature (°C)	Pressure (kPa)	Temperature (°C)	Pressure (kPa)
V-101	48.3	2996.8	130.9	2962.3
V-102	46.5	791.3	117.2	1311.5
V-103	45.0	300.3	100.8	968.3
V-104	43.8	167.5	70.2	383.0
V-105	42.9	117.2	55.3	117.2
V-201	–	–	21.1	2927.8
V-202	–	–	21.1	1277.1
V-203	–	–	48.9	933.8
V-204	–	–	50.2	348.5
V-301	54.7	2893.4	24.1	2858.9
V-302	48.9	7793.0	48.9	9247.6
V-303	48.9	18926.1	48.9	18926.1

Figures 4-5 and 4-6 show the results of the mean objective value and the best design variables of each generation. In Case 1, the CMA-ES found the optimal value within 30 to 40 generations because of fewer numbers of design variables and the lack of a condensate recycle flow. In Case 2, as the generations increased, no more improvements with respect to the objective value were made about 250 generations iterated. As the number of function evaluation in each generation is 100 and 300 in Case 1 and 2 respectively, the number of function evaluation to find optimal solution was 3,100 and 75,000 respectively. In Figure 4-6, the variables, converged to the lower bound 0, are the condenser temperature because of the assumption to maintain the condenser temperature at or above 21.1 ˚C.

As the LP steam at 445 kPa is chosen by the optimization for feed heating, the result of temperature in a stock tank (V-105) increase of 12.4 ˚C (see Table 4-7). Since the assumption that the LP steam can heat the streams to 130.9 ˚C and resulting effluent temperature in the feed heater is 130.9 ˚C in Case 2 (see Table 4-7), the LP steam is the most profitable method for heating medium and makes the maximum use of its heating capacity from an economic aspect. Consequentially, the higher temperature in the stock tank could prevent the crude oil from vaporizing due to an increase of temperature during the daytime or summer season. Hence, the feed heater prevents the product oil loss and provides more eco-friendly crude oil with respect to an economic and

environmental point of view.

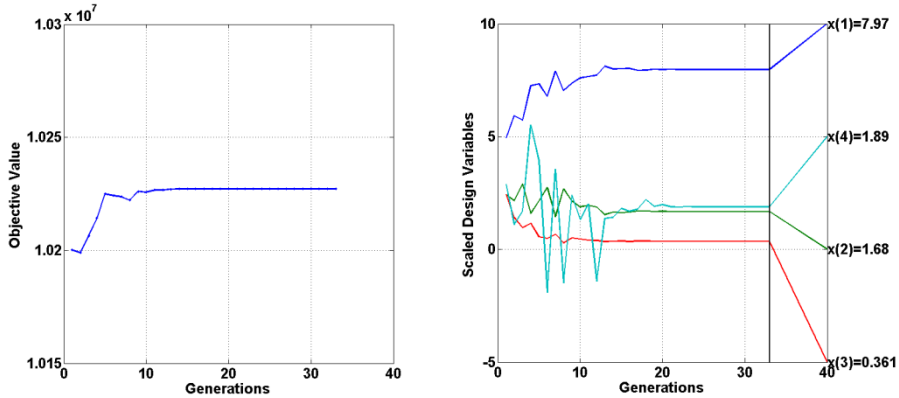

Figure 4-6 MSS optimization results of Case 1

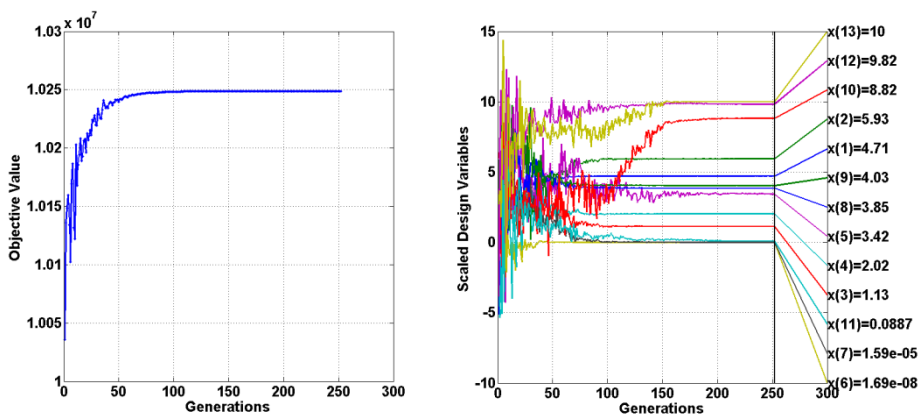

Figure 4-7 MSS optimization results of Case 2

As described in Table 4-6, the first advantage of condensate recycling is satisfying the RVP specification. Furthermore, the total profit increases by $21,660/day multistage separation process owing to the increase of oil production rate as represented in Figure 4-8, even though the RVP value decreases from 72.81 in Case 1 to 55.16 kPa in Case 2. Concerning crude oil recovery,

Second, condensate and wastewater recycling increase the operation cost. This increase is owing to the notable increase in steam, cooling water and wastewater, as shown in Figure 4-9, which are ruled out due to the acquiescence of their importance and influence on total economic evaluation in order to simplify the process model.

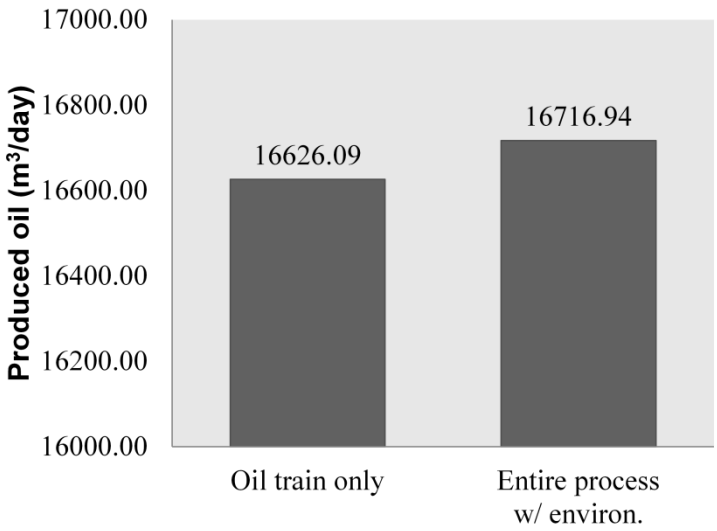

Figure 4-8 Crude oil production rate

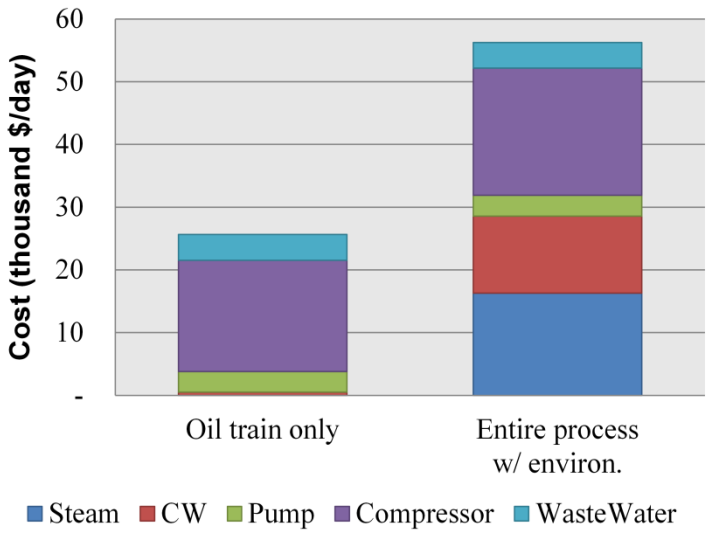

Figure 4-9 Utility cost for oil production

In Figure 4-9, the wastewater cost appears in Case 2 because it is taken into account in Case 2 only. However the cooling water cost, considered in both Case 1 and 2, remarkably increases in Case 2 as compared with Case 1. The increase in the cooling cost is owing to the increase in chilled water consumption as represented in Figure 4-10. Since the assumption that chilled water has ability to cool down the streams to 21.1 ˚C and the resulting operating temperature in the first and second condenser in Case 2 is 21.1 ˚C (see Table 4-7), it seems rational to conclude that the condensate recycling has to be made up in the early stage as much as possible to achieve the profitable process design.

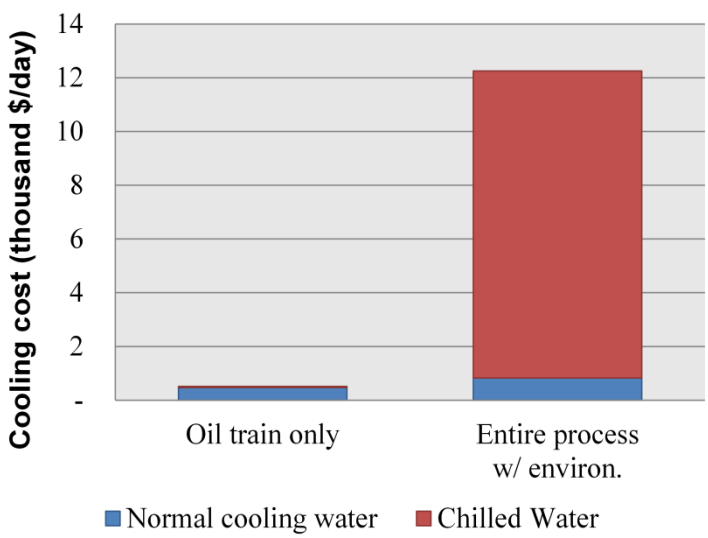

Figure 4-10 Cost of normal and chilled cooling water in two cases

Finally, according to the objective of multistage crude oil production facilities described by Abdel-Aal, et al. [42], the performance of multistage separation can be analyzed by contents of light and intermediate hydrocarbons in the crude oil. As summarized in Table 4-8, the multistage separation with the condensate and wastewater recycling process has a much better performance than just considering the oil treating train in terms of maximizing the removal of light hydrocarbons from the crude oil and the recovery of intermediate hydrocarbons into the crude oil. It is also worth noting that both profit and quality of crude oil are improved by the condensate and wastewater recycling in spite of considering environmental issues to prevent the air and ocean pollution or greenhouse gas emission.

Table 4-8 Volumetric component flows in crude oil [m^3/day]

	Case 1	**Case 2**
Light HC (C1+C2)	19.0	1.1
Intermediate HC (C3+C4+C5)	1210.6	1247.8
Heavy HC (C6+)	14862.7	14920.0

As result of this study, determining the optimal process condition considering only the production rate or operating cost with simplified process model during the preliminary design of offshore oil production facilities has no beneficial use. This study proposed an integrated solution procedure using a general-purposed process simulator for the rigorous and reliable analysis of the crude oil separation process as well as the consideration of environmental constraints, and used CMA-ES to find a simultaneous solution to this multivariable problem.

In the result shown in Figure 4-11, condensate and wastewater recycling increases profits more than increasing the number of separation stages due to the significant increase in product sales even if the increase in required operating cost. Attempting to achieve a tradeoff between the oil recovery and operating cost is essential to find global optimum of maximum profits with respecting the RVP and water contents specifications.

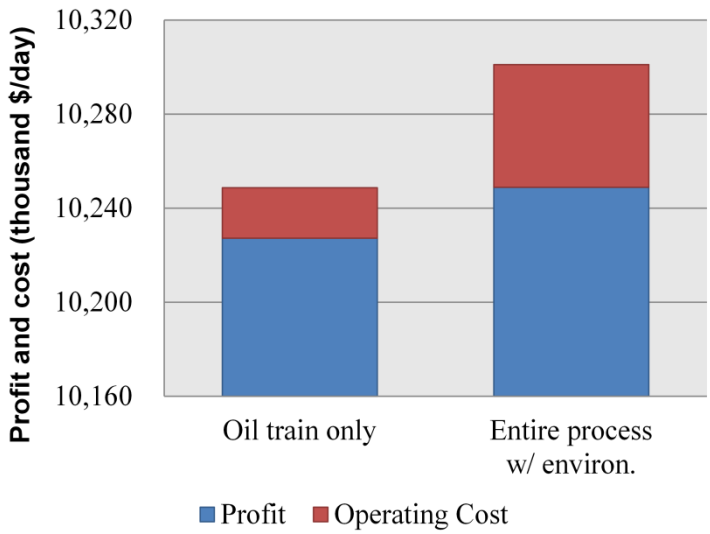

Figure 4-11 Total profit and operating cost in two case

Chapter 5. Case Study II

5.1 Integrated Inherent Risk Analysis

Preliminary design in chemical process furnishes economic feasibility through calculation of both mass balance and energy balance and makes it possible to produce a desired product under the given conditions. Through this design stage, the most profitable process should be designed to manage additional cost during the detailed design or hazard assessment later. However, in this stage, the process also possesses unchangeable characteristics, since the materials, reactions, unit configuration, and operating conditions were determined. Unique characteristics could be very economic feature, but it also implies various potential risk factors as well.

The typical design steps of a general chemical process are represented in Figure 5-1. The conceptual design is a step to come up with the result of the most profitable process design, and then, the piping and instrument diagram (P&ID) and plant layout are decided by the detail design activity. Since then, the process safety is ensured by the quantitative and qualitative risk assessment to obey the safety guides or regulations. The consequences resulting from risk assessment are 1) hazard identification, 2) layout modification, 3) analysis of safety distance for

high risk equipments, 4) emergency planning and so on [65-69]. These activities focus on external process specifications instead of changing original design or design philosophy.

Recently, chemical accidents occur with frequency in Korea and affect all other industries in various ways. The sustainability assessment in chemical industry engage public attention, and especially, quantifying and considering the risk in preliminary design stage are required to raise the sustainability of the chemical processes [70]. Therefore, it becomes extremely important to design process considering both economics and safety by integrating process simulation and quantitative risk analysis during preliminary design stage so that the preliminary design possesses the marked safety feature.

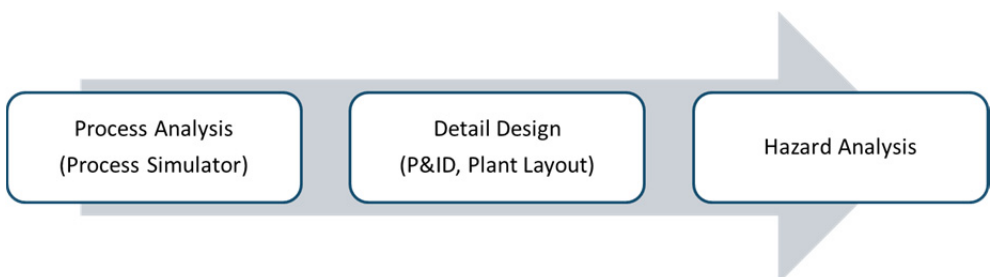

Figure 5-1 Typical design steps of chemical processes

Typical safety and risk evaluation has a practical purpose that the safety or hazard of a chemical process fulfills a certain level required by regulations or for the stable operation of the process after the detail process design. Figure 5-2 shows the steps of safety and risk evaluation is represented by Suokas and Kakko [71], and Table 5-1 presents the safety analysis techniques and their typical use introduced by CCPS [72]. The aims of safety and risk evaluation is to support the decision-making on plant layout, construction, and localization [73].

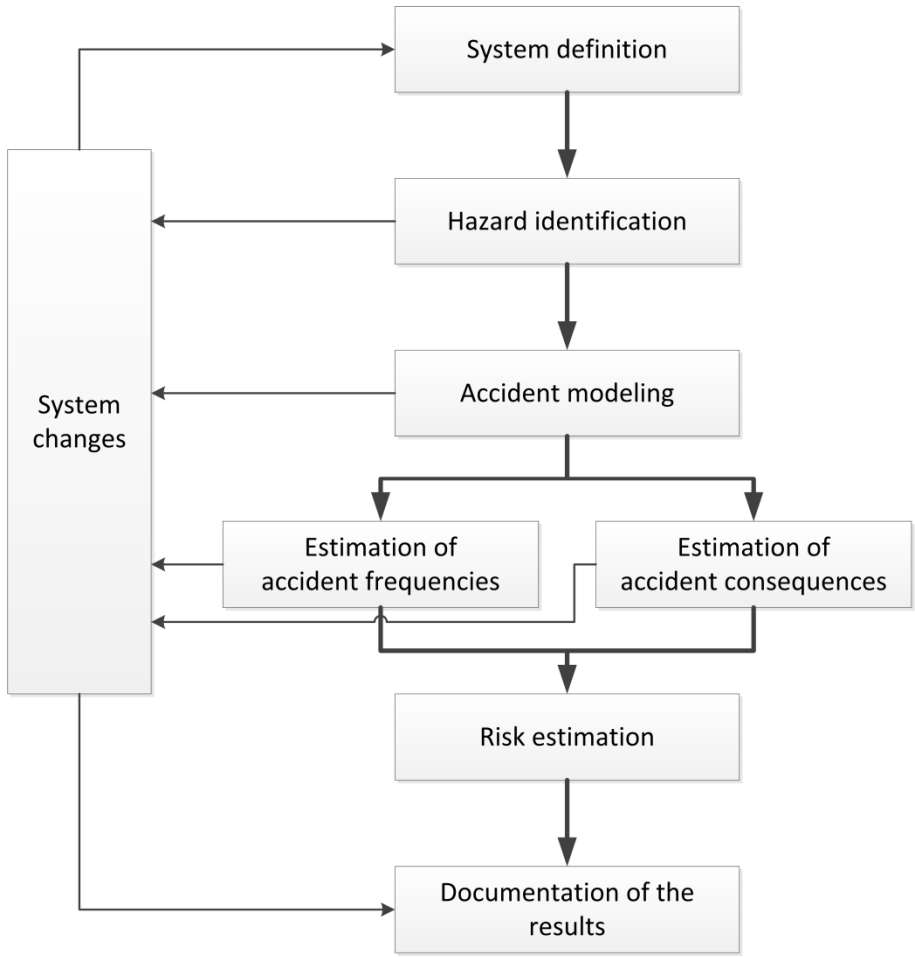

Figure 5-2 Steps of safety and risk analysis [71]

Table 5-1 Typical uses of hazard evaluation techniques [72]

	Safety Review	Checklist	Relative Ranking	PHA	What-If	What-if/Checklist	HAZOP	FMEA	Fault Tree	Event Tree	CCA	HRA
Research & Development	○	○	●	●	●	○	○	○	○	○	○	○
Conceptual Design	○	●	●	●	●	●	○	○	○	○	○	○
Pilot Plant Operation	○	●	○	●	●	●	●	●	●	●	●	●
Detailed Engineering	○	●	○	●	●	●	●	●	●	●	●	●
Construction/Start-up	●	●	○	○	●	●	○	○	○	○	○	●
Routine Operation	●	●	○	○	●	●	●	●	●	●	●	●
Expansion or Modification	●	●	●	●	●	●	●	●	●	●	●	●
Incident Investigation	○	○	○	○	●	○	●	●	●	●	●	●
Decommissioning	●	●	○	○	●	●	○	○	○	○	○	○

○ Rarely used or inappropriate ● Commonly used

Inherent risk analysis is to find technologies and chemicals that reduce or eliminate the possibility of an accident by modifying the design using different chemicals, hardware, controls, and operating conditions [74]. Inherent risk analysis can be applied during conceptual design and simulation stage to identify inherent risks and determine the inherently safer design and operation conditions whereas the traditional quantitative risk analysis is generally performed to prove or demonstrate the safety of design cases as required by regulatory guidelines after completion of detailed design. So the process design and simulation integrating with estimation of risk and consequence is essential to design the more safe process and determine operation conditions to reduce inherent risks, and the quantitative risk analysis can be helpful to assess and evaluate the inherent safety for the conceptual design of process as shown in Figure 5-3.

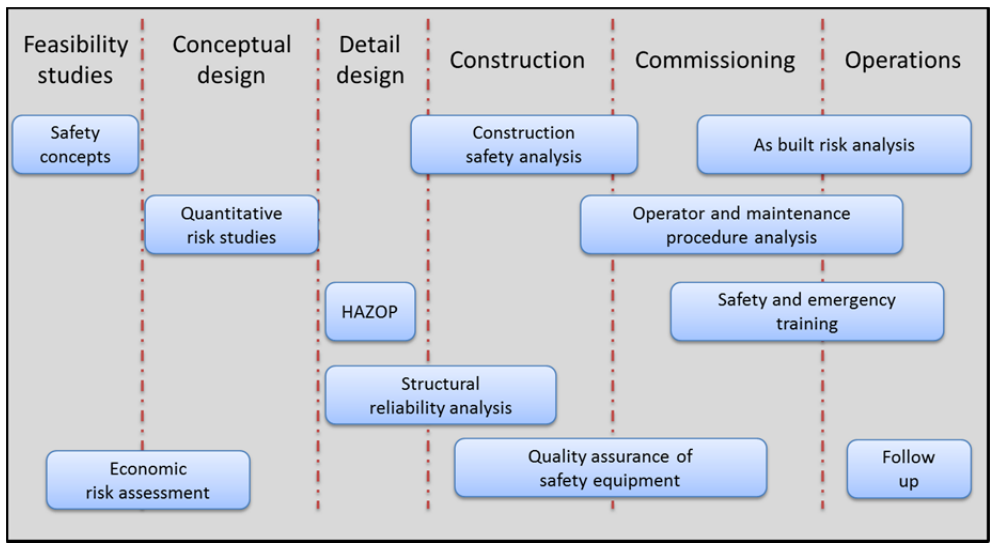

Figure 5-3 Safety analysis programs [75]

Mohd Shariff, et al. [76] presented a methodology to integrate simulation and quantitative explosion consequence analysis in the preliminary design stage, as shown Figure 5-4. In this study, the quantitative risk analysis of explosion consequence was calculated by TNT-equivalency method, and the flammable mass participated in explosion was estimated at flammable limits and gas release model. However, the study has a limitation on the systematic framework to find more safe process design.

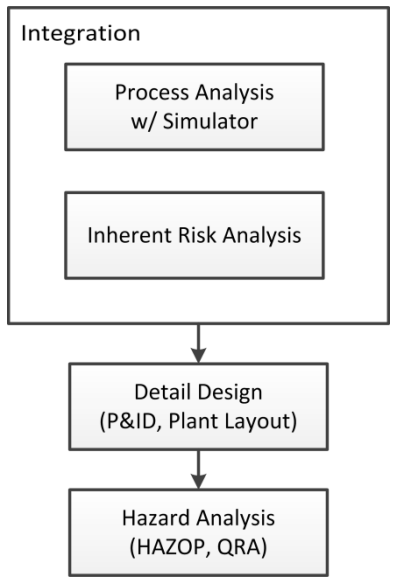

Figure 5-4 Integrated inherent risk analysis

Traditional quantitative risk assessment (QRA) has gained a wide acceptance as a powerful tool to identify and assess the significant sources of risk and evaluate alternative risk control measures in chemical process industries. QRA is a part of process safety management system (PSMS) [77] and considered as a valuable tool in decision making processes in order to quantify opinions and to combine them effectively with available statistical data. Mannan [78] concluded that QRA is an element that cannot be ignored in decision making about risk as it is the only discipline capable of enabling a number to be applied and comparisons to be made in quantitative manner.

Although the IRA adopts the methodological approach from the QRA, the two methodologies have fundamental differences. The key difference is the stage when the methods are performed. Traditional QRA is performed after a detailed engineering for equipment sizing, P&ID drawing and plant layout arrangement has been completed, since the QRA requires these informations. Contrastively, the IRA is proposed to be used as early as preliminary design with the process simulation, it determines process configuration as well as heat and material balances. The IRA does not take into consideration the safety control instruments or procedures to protect the system against any accident or hazard of process. The detailed similarity and comparison between QRA and IRA is summarized in Table 5-2 presented by Shariff and Leong [79].

In particular, for the offshore platform, the NORSOK standard, developed by the Norwegian petroleum industry, is a principle standard for offshore structures, referring to ISO 19900, '*Petroleum and natural gas industries – General requirements for offshore structures*'.[80-83] However, the NORSOK is a kind of goal of the QRA activity because it is developed to ensure adequate safety regulations and guidelines. So the methodology, adopted for identifying process safety in this study, is different from the approach of the NORSOK standard with respect to the purpose and measure of implementation.

Table 5-2 Comparison of QRA and IRA

Criteria	QRA	IRA
Stage to be applied	• After completion of detailed engineering design • To demonstrate or prove "safety case" as required by regulatory agencies	• During preliminary design/simulation stage • To proactively identify inherent risk to the design • To guide risk reduction by adopting inherent safety and principles
Regulatory requirements	• Required by regulatory agencies e.g.) NORSOK	• No regulatory requirement
Information required	• P&ID • Detailed historical weather data	• Simulation data • Predicted piping and equipment sizing
Scenario	• Only few credible scenario to be studied in detail	• Basic scenario such as pipe and equipment leak
Duration of analysis	• Relatively long • Ranging from 40 to 15000 man-hours	• Relatively quick as it is carried out in parallel with simulation work

5.2 Dual Mixed Refrigerant Natural Gas Liquefaction Process

5.2.1 Process Description

Using hydrocarbon mixture refrigerant for liquefaction of natural gas has the advantage that it can overcome the low efficiency of the systems operating with pure component fluids for liquefaction. So the mixed refrigerant process is possible to be constructed with large capacity and low cost. For instance, the Linde-Hampson refrigeration process, consisting of a set of heat exchanger, throttling valve, compressor and condenser, is a good example to compare the performance with pure component and hydrocarbon mixture refrigerants due to its simplicity, and the comparison results of the process operating with pure and mixture hydrocarbons are summarized in Table 5-3 [84]. Putting some other interpretation on the advantage in using hydrocarbon mixture refrigerant, the most essential unit operation in a liquefaction process is the heat exchangers to cool the natural gas down. Since the natural gas is a hydrocarbon mixture, its liquefaction occurs at a sliding temperature interval. Using the mixture refrigerant in the LNG process, the cold composite curve can be nicely matched to the hot composite curve so that the efficiency of refrigeration cycle is enhanced [19].

Table 5-3 Comparison of Linde-Hampson refrigerators with pure fluids and typical nitrogen-hydrocarbon mixtures [84]

	Refrigerant type	
	Pure	**Mixture**
Typical operating pressures	100~200 bar	15~20 bar
Refrigeration temperature at evaporator pressure of 1 bar	77.24 K	78~79 K
Entropy change during heat addition process	Small	Large
Heat transfer coefficients in heat exchanger	Small	Large
Temperature approach at cold end of the heat exchanger	Large, typically 70~90 K	Small, typically 5-15K
Theoretical exergy efficiency	10~20 %	30~40 %
Practical exergy efficiency	1~2 %	3~6 %

The dual mixed refrigerant (DMR) natural gas liquefaction process is one of the candidates for applying to the offshore platform, as shown in Figure 5-5. It has two mixed refrigerant cycles, consisting of methane (C_1), ethane (C_2), propane (C_3), butane (C_4) and nitrogen (N_2), for precooling (101~110) and condensing or subcooling (201~217).

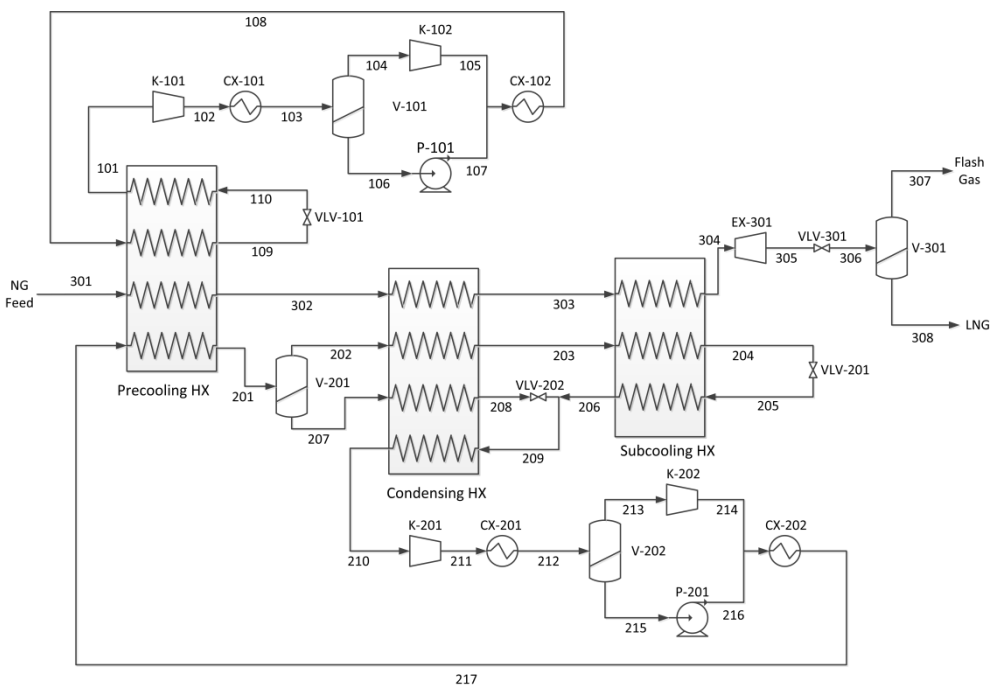

Figure 5-5 DMR process with the precooling refrigerant evaporated at a single pressure

Compared with C_3MR, the mixed refrigerant, used as the precooling refrigerant instead of pure fluids such as propane (C_3), saves the compression power due to the same reason described above [85]. A main argument for developing the DMR process is the need for a pre-cooling refrigerant that can cover a wider temperature range than pure component refrigerant such as propane. In Figure 5-5, the precooling refrigerant is evaporated at a single pressure in the precooling heat exchanger (Precooling HX).

The number of design variables for the DMR process, illustrated in Figure 5-5, is twenty two. They are 1) six of MR pressure values in stream 102/108/110/205 /211/217, 2) four of condenser temperature values in CX-101/102/201/202, 3) ten of MR composition values in two refrigerant cycles, and 4) two of natural gas effluent temperature in stream 302/303. The design specification is the final temperature of liquefied natural gas in stream 304, and the constraints are 1) minimum temperature approaches in three LNG heat exchangers (Precooling/ Condensing/Subcooling HX) and four condensers (CX-101/102/201/202), and 2) the compressor suction flow requirement of keeping the single vapor phase without liquids in stream 101/210. The design specification and assumptions are summarized in Table 5-4 and the natural gas feed composition is shown in Table 5-5.

Table 5-4 Design specification and assumptions for DMR process modeling

Min. Temp. Approach in LNG HX	3 ˚C
Min. Temp. Approach in condenser	5 ˚C
Pressure drop in LNG HX	50 kPa only for hot stream
Pressure drop in condenser	200 kPa only for hot streams
Adiabatic efficiency of centrifugal compressors	75 %
Adiabatic efficiency of pumps	75 %
Natural gas feed operating condition	20 ˚C and 6000 kPa
LNG target temperature	-153.1 ˚C

Table 5-5 Natural gas feed composition

Component	Component mass flow (kg/s)	Mole fraction
Methane (C_1)	76.32	0.888
Ethane (C_2)	9.02	0.056
Propane (C_3)	8.74	0.037
Butane (C_4)	5.92	0.019
Total	100.00	1.000

The Honeywell UniSim is used for simulation of the DMR process with the Peng-Robinson equation of state model recommended in case of minimum -271 ˚C and maximum 100,000 kPa process condition. The cost of normal cooling water and electricity is calculated by the Figure 4-4 [63].

The upper and lower bounds of design variables for optimization are described in Table 5-6. It is noteworthy that the medium pressure in two-stage compression is expressed by the fraction between low and high pressure of compression so that the medium pressure never go outside the bounds and it can helpful to make the convergence of simulation easier. So the fraction, zero means that medium pressure is same as low pressure and one means the high pressure.

Table 5-6 Upper and lower bounds of design variables

Stream	Design variable	Lower bound	Upper bound
MR1 & MR2	N_2 mass flow (kg/s)	0.0	350.0
	C_1 mass flow (kg/s)	0.0	350.0
	C_2 mass flow (kg/s)	0.0	350.0
	C_3 mass flow (kg/s)	0.0	350.0
	C_4 mass flow (kg/s)	0.0	350.0
	Outlet temp in 1st cooler (°C)	30.0	45.0
	Outlet temp in 2nd cooler (°C)	30.0	45.0
	Low pressure (kPa)	1.5	30.0
	Medium pressure (fraction)	0.0	1.0
	High pressure (kPa)	5.0	100.0
NG	Precooled NG temp (°C)	-100.0	20.0
	Condensed NG temp (°C)	-135.0	0.0

5.2.2 Issues on Offshore LNG Safety

Nature gas liquefaction technologies have either pure, mixed or cascade refrigerant cycles. The number of cycles varies from one to three, depending on its success of an efficient liquefaction. Table 5-7 presents the important criteria to select the type of a natural gas liquefaction process [85]. Up to now, the expander processes, such as N_2-Expander and Niche LNG, are regarded as the most suitable ones for an offshore environment. However, due to the demand for large capacity offshore LNG process, the MR processes cannot be ignored because the cascade process, among the alternative processes, has too many equipments to be installed at offshore platform than the MR processes. Approximatively, the capacity of the MR processes is 4~8 MTPA, while the capacity of N_2-Expander is 1.5~2.5 MTPA. As a result, if it would be possible to overcome the safety issues, the DMR and C_3MR are regarded as the most likely processes for the large capacity LNG plant at offshore. And the DMR process is more suitable than C_3MR since the precooling configuration of the DMR process is more compact than C_3MR as well as all the specific power, power consumption and refrigerant inventory are lower than other technology [86].

Table 5-7 Liquefaction processes suitability for offshore platform [85]

Category	Technology	Cascade	C_3MR DMR	SMR	N_2-Exp	Niche LNG
Suitability to LNG FPSO	Equipment count for liquefaction	50~65	45~65	40~55	12	11
	Process sensitive to motion	Yes	Yes	Yes	No	No
	Ease of start-up /operation	Low	Low	Low	High	High
	Flexible to feed gas changes	Medium	Low	Low	High	High
Safety issues	Storage of HC refrigerants	Yes	Yes	Yes	No	No
	Cryogenic equipment count	High	High	Medium	Low	Low
	Space requirement	High	High	Medium	Low	Low
Efficiency	Thermal Efficiency (% of HHV)	91%	92%	89%	84%	89%
	Availability	Medium	Medium	Medium	High	High
	Specific investment	High	High	Medium	Medium	Low

5.2.3 Integrated Inherent Safety Assessment

In order to assess the inherent safety of the DMR process, the inherent safety explosion consequence is estimated as shown in Figure 5-6.

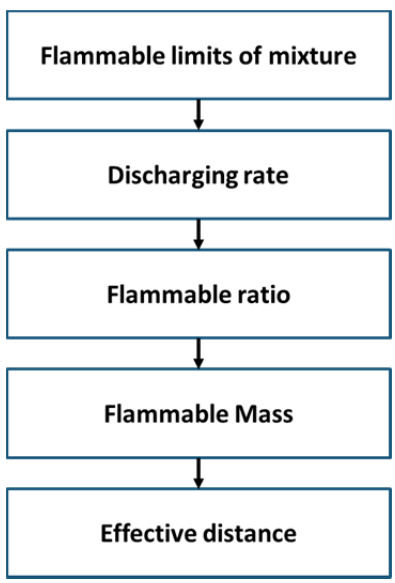

Figure 5-6 Estimation procedure of inherent explosion consequence

The inherent safety assessment, proposed in this case study, is originally based on the integration of process simulator and quantitative risk analysis. Since the safety and economics has an opposite relation, Shah, et al. [87] attempted to

show the relation between these two objectives using the multiobjective optimization with respect to the cost and inventory of refrigerant. However, as the mass of hazard materials is not in direct proportion to real risk or accident consequence, the estimation based on quantitative risk analysis can be a powerful guide to show the inherent safety level precisely.

The safety issue to adopt MR process at offshore platform is of importance in the engineering and construction of LNG process and the major accident type is explosion. So the integrated inherent safety assessment in Figure 5-6 is to estimate the real explosion consequence from leaking of pressurized gas and liquid phase of light hydrocarbons.

5.3 Problem Statement

5.3.1 (Case 1) Operating Cost Minimization

Operating cost consists of cooling water cost for the condensation and electric cost for the pressurization. In order to assure the process availability, the minimum temperature approach in every heat exchanger should be satisfied with its specification and the vapor phase fraction requirement in suction flow of every compressor has to be considered as shown in following equation.

$$\begin{aligned} &\min . \ f_{cost}(x) = f_C(x) + f_E(x), \ \ x \in \mathbb{R}^n \\ &\text{s.t.} \begin{cases} \Delta T_{\min,i} \geq t_{spec}, & (i = 1, \cdots, k) \\ F_{vap,j} = 1, & (j = 1, \cdots, l) \end{cases} \end{aligned} \tag{13}$$

5.3.2 (Case 2) Explosion Consequence Minimization

In this study, the explosion consequence is defined by the estimated distance to 1 psi overpressure for vapor cloud explosion as shown in Chapter 5-2. Even though it is possible to make the process safer, the economics should not be neglected because it is the reason for the process. Thus the explosion consequence minimization should be conducted by considering the economics as

an optimization constraint. The following equation represents the explosion consequence minimization likewise the operating cost minimization. In order to consider the process economics, the operating cost should be satisfied within the allowed cost.

$$\begin{aligned} &\min.\ f_{\exp losion}(x),\ \ x \in \mathbb{R}^n \\ &\text{s.t.} \begin{cases} \Delta T_{\min,i} \geq t_{spec}, & (i = 1, \cdots, k) \\ F_{vap,j} = 1, & (j = 1, \cdots, l) \\ f_{cost} \leq \text{Cost}_{allowed} \end{cases} \end{aligned} \tag{14}$$

5.4 Framework for Inherent Risk Identification

5.4.1 Flammable Limits of Mixture

The lower flammable limit (*LFL*) and upper flammable limit (*UFL*) for mixture are the basis to determine explosion consequence, and they can be estimated by Le Chatelier's rule as following equations [88]:

$$LFL = \frac{\sum y_i}{\sum (y_i / LFL_i)}, \quad UFL = \frac{\sum y_i}{\sum (y_i / UFL_i)}. \tag{15}$$

LFL_i and UFL_i are the lower and upper flammable limits of pure component *i*,

and y_i is the mole% of pure component i in gas mixture. The lower and upper flammable limits of pure components involved in this study are summarized in Table 5-8 [60].

Table 5-8 Lower and upper flammable limits of pure components

Component	**LFL (mol% in air)**	**UFL (mol% in air)**
Methane	5.0	15.0
Ethane	2.9	13.0
Propane	2.0	9.5
Butane	1.5	9.0

5.4.2 Discharging Rate of Gas Release

The equation for estimating release rate of a gas from a hole is based on the equation for gas discharge rate in CEPPO [89]. This gas discharge rate model is different in choked or non-choked flow conditions. Choked flow condition satisfies following inequality expressed in a ratio comparison of system pressure, atmospheric pressure, and critical pressure of mixture [76]:

$$\frac{P_{atm}}{P} < \frac{P_c}{P}. \tag{16}$$

Total mass resealed in choked and non-choked condition can be calculated using Eq. (17) and (18), respectively.

$$\dot{m} = c_d A_h \sqrt{k \rho P \left(\frac{2}{k+1} \right)^{\frac{k+1}{k-1}}} \tag{17}$$

$$\dot{m} = c_d A_h \sqrt{2 \rho P \left(\frac{k}{k-1} \right) \left[\left(\frac{P_{atm}}{P} \right)^{\frac{2}{k}} - \left(\frac{P_{atm}}{P} \right)^{\frac{k+1}{k}} \right]} \tag{18}$$

The discharging coefficient (c_d) is 0.975 for gases and 0.61 for liquids. For vapor-liquid flows, c_d increases from 0.61 to 0.975 as vapor fraction increases from 0 to 1 [76]. In addition, the opening area (A_h) and density (ρ) are required

for Eq. (17) and (18).

5.4.3 Ratio of Flammable Mass to Total Discharging Mass

From a flammable mass from passive dispersion models, the dispersion or air entrainment rate for a Gaussian model is expressed inherently by the increase cloud dimensions [88, 90]. From this model, the ratio of actual flammable mass to total discharging mass can be estimated by Eq. (19) where C_s and C_{LFL} is mass concentration of system and lower flammable limit, respectively.

$$\frac{\dot{m}_f}{\dot{m}} = erf\left[\sqrt{\ln\left(\frac{C_s}{C_{LFL}}\right)}\right] - \frac{2C_{LFL}}{C_s\sqrt{\pi}}\left[\sqrt{\ln\left(\frac{C_s}{C_{LFL}}\right)}\right] \tag{19}$$

In the worst scenario case, maximum value of flammable ratio is reached when the following equation is satisfied where C_{UFL} is mass concentration of upper flammable limit [88, 90]:

$$lnC_s = \frac{C_{UFL}^2 lnC_{UFL} - C_{LFL}^2 lnC_{LFL}}{C_{UFL}^2 - C_{LFL}^2}. \tag{20}$$

5.4.4 Effective Distance from Total Flammable Mass

From CEPPO [89], consequence distance to an overpressure of 1 psi can be determined using following equation, which is based on the TNT-equivalency method and the assumption of maximum ratio of flammable mass with an instantaneous discharging time:

$$D = 17\left(t_{Release}\dot{m}\frac{HC_f}{HC_{TNT}} \right)^{1/3}. \tag{21}$$

The leaking scenario is assumed to originate from 2.5 cm diameter hole on the pipes and the response time to detect and stop the leak is estimated to be 5 min. Leak diameter is chosen based on recommendation from control of industrial major accident and hazard reported by Profession Loss Control [91]. This type of leak can result from human error, flange failures, and so on. Hydrocarbons from the pipe would leak to ambient conditions.

5.5 Process Stream Index

The Process Stream Index (PSI), used in this thesis, originally was introduced by Heikkilä [73] in order to assess the inherent safety level. It is used to represent the explosiveness of the stream considering each substance within the stream as individual components. The modified PSI is presented by Shariff, et al. [92] as described in Eq. (22).

$$\begin{aligned}
\text{PSI} &= f(\text{density, pressure, energy, combustibility}) \\
&= A_0 \times (I_p \times I_\sigma \times I_e \times I_{FL}) \\
\text{where, } I_p &= \frac{\text{pressure value of individual stream}}{\text{average pressures of all streams}} \\
I_\sigma &= \frac{\text{density value of individual stream}}{\text{average density of all streams}} \\
I_e &= \frac{\text{heating value of individual stream}}{\text{average heating value of all streams}} \\
I_{FL} &= \frac{\Delta\text{FL of individual stream}}{\text{average } \Delta\text{FL of all streams}}
\end{aligned} \tag{22}$$

The combustibility is determined as the difference in flammability limits using Eq. (15). The PSI can be applied to compare and prioritize the level of inherent safety of an individual stream against the overall stream in the simulation as shown in Figure 5-9 [92]. It is also very useful to reduce the calculation load because it can select the target streams evaluated by inherent risk analysis.

Table 5-9 PSI results of DMR process

Stream number	Heating value	Density	Pressure	△FL	PSI
208	1.02	3.83	1.83	1.02	7.29
207	1.02	2.95	1.93	1.02	5.92
204	0.94	3.24	1.73	1.10	5.81
203	0.94	2.98	1.83	1.10	5.66
109	1.01	3.71	0.79	0.94	2.77
107	1.00	3.45	0.91	0.86	2.70
201	1.01	1.19	1.93	1.04	2.41
106	1.00	3.45	0.53	0.86	1.56
220	1.01	0.38	2.03	1.04	0.82
202	0.94	0.33	1.93	1.10	0.66
219	1.01	0.30	2.06	1.04	0.64
216	1.01	0.30	2.06	1.04	0.64
110	1.01	0.63	0.89	0.94	0.53
108	1.01	1.97	0.28	0.94	0.52
215	1.01	0.18	1.11	1.04	0.21
214	1.01	0.18	1.11	1.04	0.21

105	1.02	0.19	0.91	0.99	**0.18**
213	1.01	0.14	1.13	1.04	**0.16**
209	1.02	0.83	0.14	1.02	**0.12**
205	1.01	0.20	0.53	0.94	**0.10**
103	0.94	0.59	0.15	1.10	**0.09**
102	1.01	0.12	0.55	0.94	**0.06**
104	1.02	0.12	0.53	0.99	**0.06**
210	1.01	0.19	0.14	1.04	**0.03**
101	1.01	0.06	0.26	0.94	**0.02**
206	0.94	0.04	0.14	1.10	**0.01**
211	1.01	0.02	0.12	1.04	**0.00**
212	1.01	0.02	0.12	1.04	**0.00**
217	1.01	0.00	1.11	0.91	**0.00**
218	1.01	0.00	2.06	0.91	**0.00**
Average	1.00	1.00	1.00	1.00	**1.20**

From the Table 5-9, the potentially risky streams, which are above average of PSI, are selected as shown in Figure 5-7. Especially, since the PSI scores of stream 203 and 207 are always lower than the scores of stream 204 and 208 respectively, they are counted out from the target streams set to be evaluated.

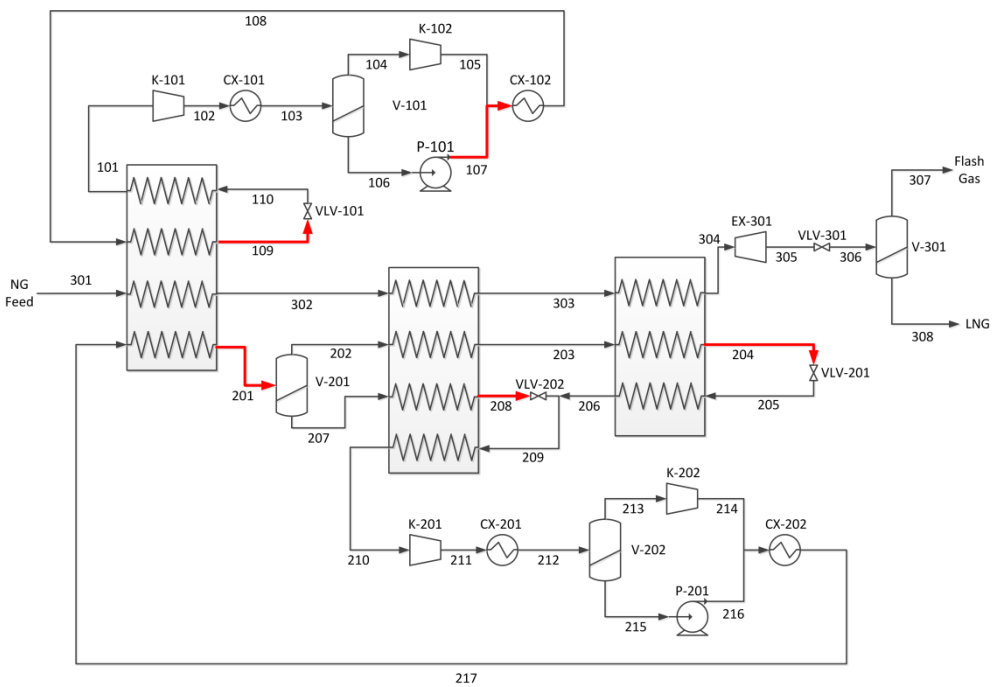

Figure 5-7 Selected risky streams (107, 109, 201, 204 and 208) based on PSI criteria

5.6 Solution Procedure

This study consists of two cases described in Chapter 5.3. The optimization for determination of minimum operating cost is a basis of assessment for safety reduction because the operating cost should be increase by the safety assurance. And then, effective distance as an explosion consequence can be minimized as the operating cost allows 0.5~20% increase from the minimum operating cost.

Overall solution procedure is shown in Figure 5.8. The CMA-ES is operated with 300 populations, and the bounds of all design variables are scaled to [0, 10] and [0, 100] by affine transformation in case of cost and safety optimization respectively. The process model is solved by Honeywell UniSim and the evaluation of objective value with CMA-ES is controlled by Matlab. The solution iteration in Figure 5-8 stops when the results of the CMA-ES satisfy the conditions presented in Table 4-5.

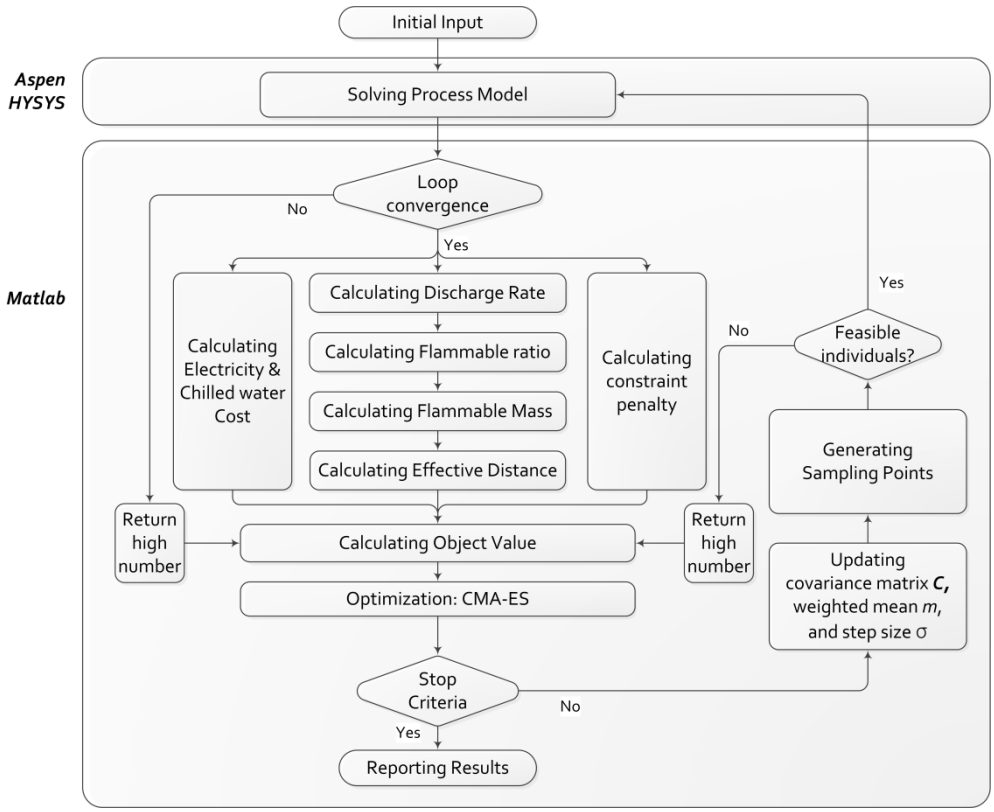

Figure 5-8 Solution procedure for optimizing LNG plant regarding inherent risk of process

5.7 Results and Discussion

Figure 5-9~15 show the results of the mean objective value and the best design variables of each generation of the CMA-ES. In all cases, the CMA-ES found the optimal value within 600 to 800 generations only (180000 to 240000 function evaluations) although the number of design variables determined by optimization is twenty two. And all the results of the values of objectives and design variables are summarized in Table 5-10.

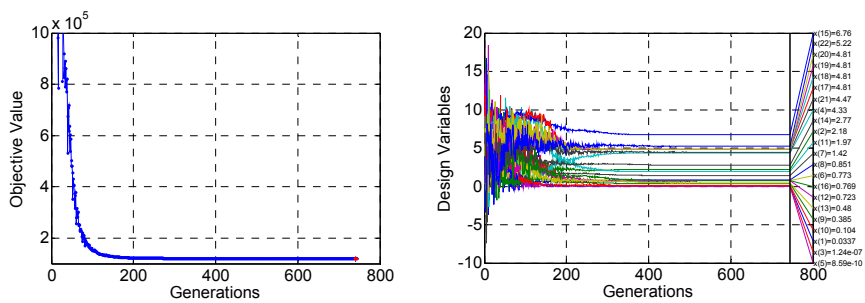

Figure 5-9 CMA-ES results of cost optimization

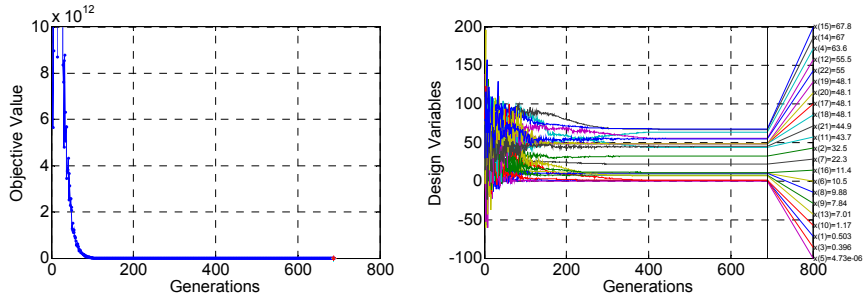

Figure 5-10 CMA-ES results of safety optimization allowing the cost increase by 0.5% of minimum operating cost

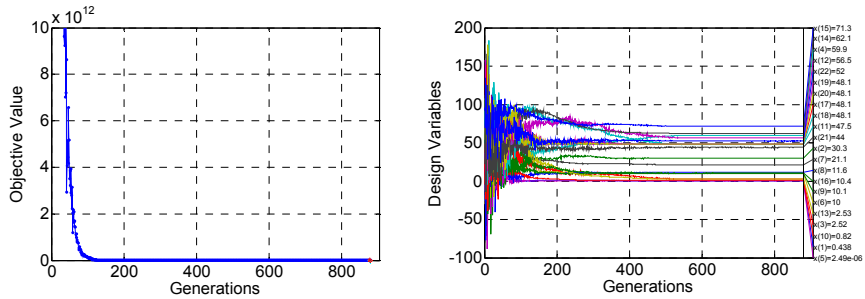

Figure 5-11 CMA-ES results of safety optimization allowing the cost increase by 1.0% of minimum operating cost

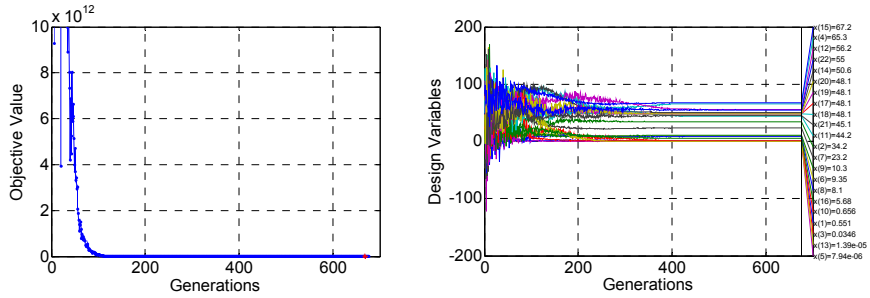

Figure 5-12 CMA-ES results of safety optimization allowing the cost increase by 3.0% of minimum operating cost

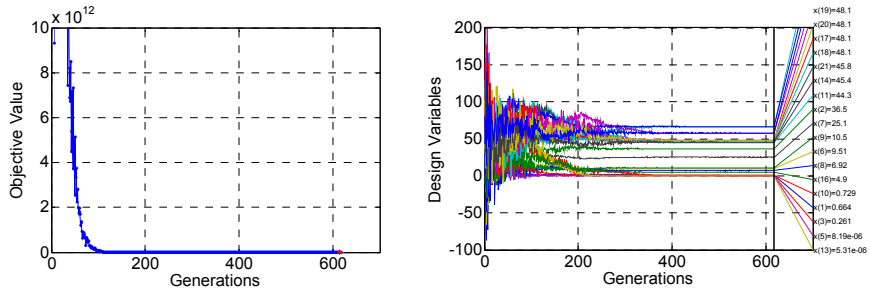

Figure 5-13 CMA-ES results of safety optimization allowing the cost increase by 5.0% of minimum operating cost

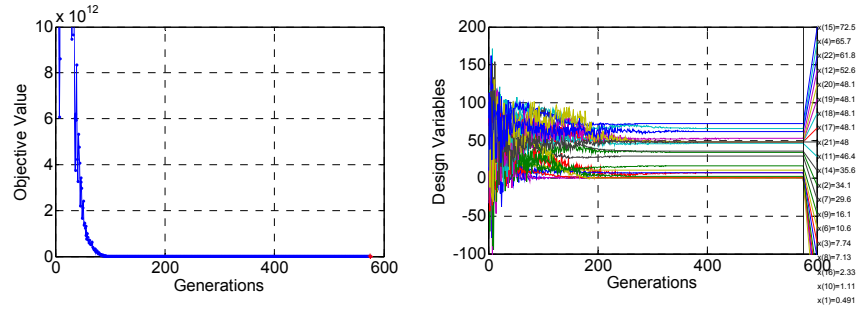

Figure 5-14 CMA-ES results of safety optimization allowing the cost increase by 10.0% of minimum operating cost

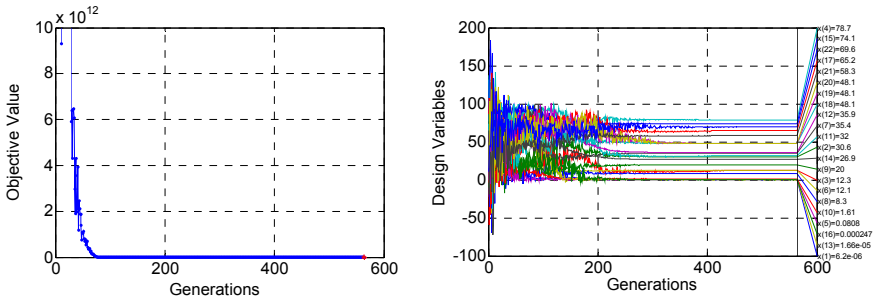

Figure 5-15 CMA-ES results of safety optimization allowing the cost increase by 20.0% of minimum operating cost

Table 5-10 Result of design variables and objective value

		Cost opt.	**Safety opt.**		
Obj.	Cost ($/day)	121240	122453	127302	145488
	Effective distance (m)	454	438	416	380
MR1 MR2	N2 (kg/s)	0 5	0 3	0 3	0 6
	C1 (kg/s)	2 39	2 39	2 35	2 33
	C2 (kg/s)	109 71	106 74	128 88	107 124
	C3 (kg/s)	0 43	9 41	1 24	43 29
	C4 (kg/s)	217 19	210 35	233 37	275 70
	LP (kPa)	515 239	553 172	527 150	422 150
	MP (kPa)	1087 2228	1113 1757	1132 1478	917 1134
	HP (kPa)	1795 4051	1824 3220	1849 2432	1270 150
	1st cooling (°C)	37.2 37.2	37.2 37.2	37.2 37.2	39.7 37.2
	2nd cooling (°C)	37.2 37.2	37.2 37.2	37.2 37.2	37.2 37.2
NG	Precooled (°C)	-32.4	-28.7	-34.0	-25.9
	Condensed (°C)	-127.7	-125.1	-130.4	-135.0

To discuss the results, Figure 5-16 shows the effective distance by explosion versus operating cost and Figure 5-17 represents the cost effectiveness of risk reduction. Effective distance is in inverse proportion to operating cost. As the cost increases from $606/day to $24,248/day, the effective distance by explosion decreases by 11 m to 74 m respectively. The cost effectiveness, represented by cost increase per amount of decrease of effective distance, becomes poor as larger amount of decrease of effective distance.

MR2 has more inherent risk by explosion than MR1 when the operating cost is less than $133,364/day. However, as the operating cost increases to more than $133,364/day, the effective distances by explosion of MR1 and MR2 are equalized.

In order to identify the key variables to reduce effective distance, Figure 5-18 and Figure 5-19 show the pressures and flow rates of MR1 and MR2. From the figures, it is clear that high pressure of MR2 is a key variable to reduce the effective distance by explosion. The high pressure of MR2 is changes from 4051 kPa to 1564 kPa. On the other hand, the flow rates of MR1 and MR2 are increased to compensate the condition of lower operating pressure. MR1 flow rate increases by 3 to 30 % and MR2 flow rate increases by 2 to 53 %.

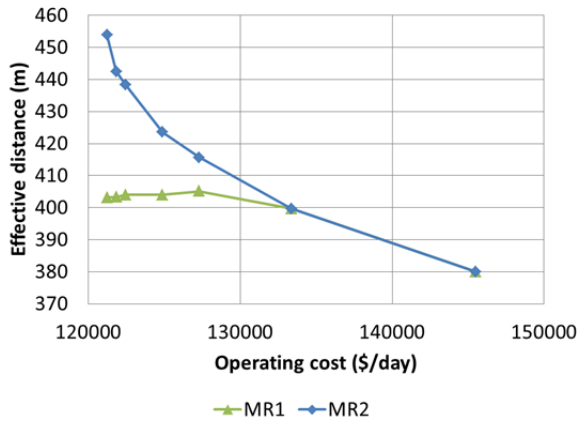

Figure 5-16 Effective distance versus operating cost

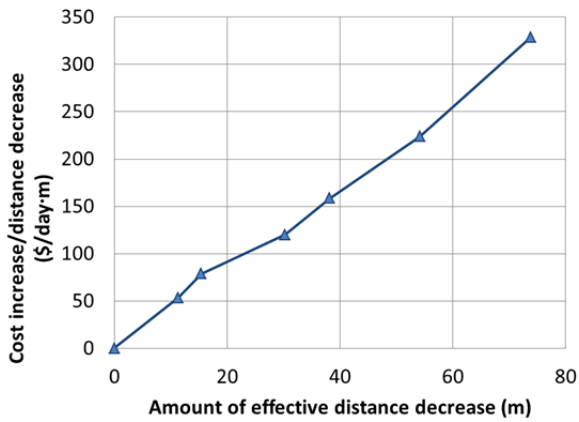

Figure 5-17 Cost increase per distance decrease versus amount of effective distance decrease

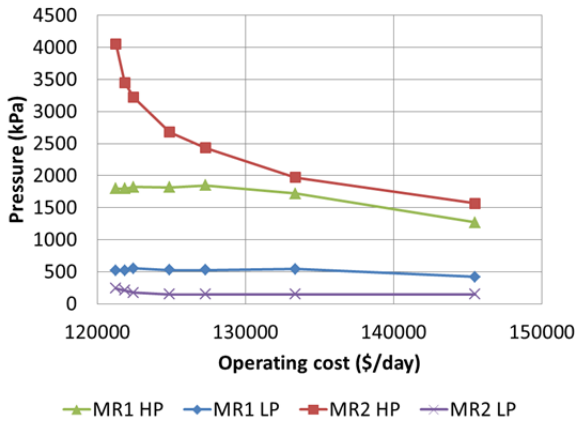

Figure 5-18 Operating pressure of MR versus operating cost

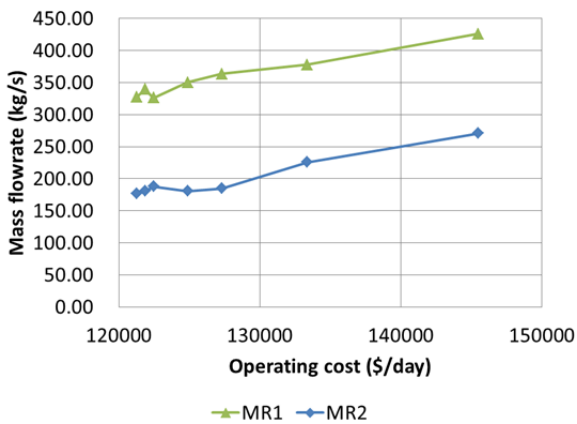

Figure 5-19 Mass flowrate of MR versus operating cost

To confirm the validity of proposed framework for inherent risk identification in Chapter 5.4, the discharge rates and effective distances of five selected streams are shown in Figure 5-20 and Figure 5-21. The discharge rate is correlated with inventory or system pressure, and the calculated effective distance reflects the effect of substances species and its composition of flammable mixture.

From the Figure 5-20 and 5-21, the stream 208 is the most danger stream in all case. And if the operating cost increases to more than $133,364/day, stream 208 of MR2 and stream 107 of MR1 are equalized. The risk by explosion of all streams decreases similarly.

Discharging rate and effective distance show similar trends. The stream 107 and 109 of MR1 are more danger than the stream 204 of MR2, when the operating cost varies between $122,453/day and $127,302/day.

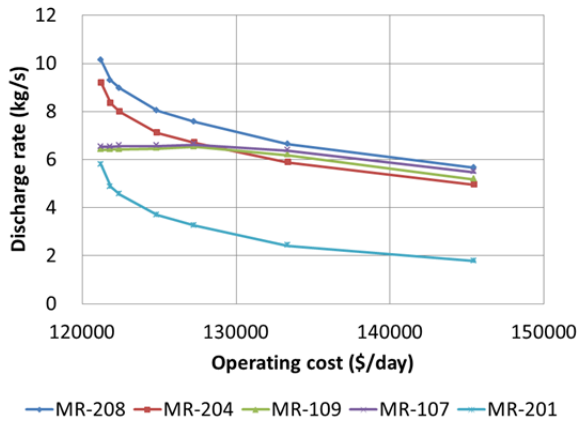

Figure 5-20 Discharge rate of selected streams versus operating cost

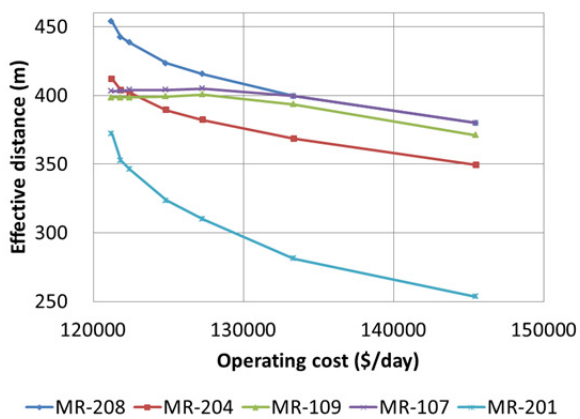

Figure 5-21 Effective distance of selected streams versus operating cost

Chapter 6. Conclusion

6.1 Summary and Contribution

This thesis has attempted to establish the methodology to define the sustainability in process design and integrate the commercial sequential modular simulator into the statistical black-box optimization method in order to consider the economic and sustainable performances.

The general-purposed sequential modular simulator is used to make the analysis and designing of the process convenient and reliable. To overcome the limitation of application of optimization using sequential modular simulator, the CMA-ES is adopted to make the procedure more accurate and faster since it has excellent ability to solve the non-convex, non-linear and discretized optimization problem with fewer evaluations of object values. Moreover, the CMA-ES can deal with the problem including a large number of design variables simultaneously so that the problem can cover the sustainability of the process as well as economics. To enhance the time complexity of the procedure, the rejection method and penalty method are adopted to avoid the infeasible simulation and unsatisfaction of process constraints.

Two case studies, related to offshore oil production facility and natural gas

liquefaction process, are conducted to verify and demonstrate the effectiveness and usefulness of the proposed solution procedure. The most profitable operating condition of an offshore oil and gas production process is successfully determined with the environmental consideration based on the entire process modeling. Furthermore, in order to make the offshore DMR process inherently safer, the risk of explosion is quantified and integration of inherent risk into economic analysis makes it possible to monitor the numerical risk factors and evaluate the safer process design.

As a result of this thesis, the proposed methodology makes it possible to design the sustainable chemical processes. It is expected to be practical and useful in designing the sustainable process since the sustainability factors in the process can be numerically monitored during preliminary process design stage using process simulator. Furthermore, it contributes to decrease various uncertainties during the process lifetime and minimize the risk and further expenses regarding the economic, environmental and safety aspects.

Based on the proposed framework and methodology in this thesis, it is applicable to the other process design problems as follows:

1) Design problems incorporated in discrete decision parameters

2) Complex processes composed of a large number of variables to be determined simultaneously

3) Optimization of the process models represented in the sequential modular simulator in order to make the steady-state analysis easy and convenient.

4) Expansion of process boundary in order to consider sustainability including economic, environmental and social aspects and confirm the more realistic results assisting the sustainable decision-making.

6.2 Future Work

There are several directions and comments for the further works to improve the results of this thesis.

1) The proposed method in this thesis is focused on the integrated sustainable process design procedure. However, the most problems, related to sustainability, often contain the conflict objectives and it would be necessary to use the multiobjective optimization strategy to support the decision-making.

2) In this thesis, the environment and safety performance is integrated into typical economic analysis and optimization. The attempt of integration and quantification of the other aspect involved in sustainability is necessary.

3) This thesis covers not the process synthesis but the process condition optimization. To apply the problem related to the process synthesis, mixed integer non-linear programming is adopted to solve the problem involved with process superstructure.

Nomenclature

A_h : Opening area [m^2]
$\boldsymbol{C}^{(g)}$: Covariance matrix at generation g
c_d : Discharge coefficient
C_s : Concentration of system [kg/m^3]
C_{LFL} , C_{UFL} : Concentration of lower & upper flammable limits [kg/m^3]
d_{env} : Environmental regulations or standards
$erf(x)$: Error function
f_C : Cooling water cost
f_{Cost} : Function of operating cost
f_E : Electricity cost
$f_{explosion}$: Function of distance to an overpressure level of 1 psi [m]
f_{Obj} : Objective function
f_{profit} : Profit function
F_{vap} : Vapor fraction
h_{env} : Environmental specification
HC_f , HC_{TNT} : Heat of combustion of fuel and TNT [kJ/kg]
$\boldsymbol{I}$: Unit matrix
k : Ratio of specific heats, C_p/C_v
LFL_i , UFL_i : Lower & upper flammable limits of component i [mol%]
$\dot{m}$: Discharge rate [kg/sec]
$\dot{m}_f$: Actual flammable mass [kg/sec]
$m^{(g)}$: Mean value at generation g
P : System pressure [kPa]
P_{atm} : Atmospheric pressure [kPa]
P_c : Critical pressure [kPa]
P_{sep} : Pressure of separator

$P_{suction}$: Suction pressure [kPa]

$P_{discharge}$: Discharge pressure [kPa]

RVP_{Oil} : Reid vapor pressure of oil [kPa]

S_{Oil}, S_{Gas} : Oil and gas sales [$/day]

$t_{Release}$: Releasing time [sec]

T_{sep} : Temperature of separator

ΔT_{min} : Minimum temperature approach [℃]

U_{CW} : Cooling water cost (normal & chilled) [$/day]

U_{Elec} : Electricity cost [$/day]

U_{STM} : Steam cost [$/day]

U_{Waste} : Wastewater treating cost [$/day]

$x_k^{(g)}$: k-th offspring from generation g

y_i : Vapor phase mole fraction of flammable component i

λ : Population size, sample size, number of offspring

μ : Number of selected search point in the population

μ_w : Weighted recombination of all μ parents selected

ρ : Density [kg/m^3]

$\sigma^{(g)}$: Step size at generation g

Abbreviations

ABACUSS	Advanced Batch and Continuous Unsteady State Simulator
AIChE	American Institute of Chemical Engineering
BPD	Barrels per Day
BS&W	Basic Sediment and Water
CCA	Cause-Consequence Analysis
CEPPO	Chemical Emergency Preparedness and Prevention Office
CMA-ES	Covariance Matrix Adaptation Evolution Strategy
DMR	Dual Mixed Refrigerant
EPA	Environmental Protection Agency
FMEA	Failure Modes and Effects Analysis
FPSO	Floating Production Storage and Offloading
GA	Genetic Algorithm
GHG	Green House Gases
GOR	Gas-Oil Ratio
GRI	Global Reporting Initiative
gPROMS	generalized Process Modelling System
HAZOP	Hazard and Operability Study (or Analysis)
HRA	Human Reliability Analysis
IChemE	Institute of Chemical Engineers
IRA	Inherent Risk Analysis
MR	Mixed Refrigerant
MSO	Modeling, Simulation and Optimization
MSS	Multi-Stage Separation
MTPA	Million metric Tonnes Per Annum
NORSOK	Norsk Sokkels Konkuranseposisjon
P&ID	Piping and Instrument Diagram
PHA	Process Hazard Analysis

PSI	Process Stream Index
PSMS	Process Safety Management System
PSO	Particle Swarm Optimization
RVP	Reid Vapor Pressure
QRA	Quantitative Risk Analysis
SI	Sustainability Index
SQP	Sequential Quadratic Programming
TNT	Trinitrotoluene
UNEP	United Nations Environmental Programme
VOC	Volatile Organic Compound

References

[1] WCED, *World Commission on Environment and Development: Our Common Future*. Oxford: Oxford Univ. Press, 1987.

[2] Damjan Krajnc and Peter Glavič, "How to compare companies on relevant dimensions of sustainability," *Ecological Economics,* vol. 55, pp. 551-563, 12/1/ 2005.

[3] Carlo Vezzoli and Ezio Manzini, *Design for Environmental Sustainability*: Springer London, 2008.

[4] Adisa Azapagic and Slobodan Perdan, *Sustainable Development in Practice*, 2nd ed. U.K.: Wiley-Blackwell, 2011.

[5] Joseph Fiksel, Tarsha Eason, and Herbert Frederickson, "A Framework for Sustainability Indicators at EPA," U.S. Environmental Protection Agency,Oct. 2012.

[6] Namjin Jang, "A Study on the Inherent Safety for Sustainable Process Design Based on Fuzzy Logic," Ph.D., Chemical and Biological Engineering, Seoul National University, Seoul, 2013.

[7] Joseph Fiksel, Tarsha Eason, and Herbert Frederickson, "A Framework for Sustainability Indicators at EPA," U.S. Environmental Protection Agency,2012.

[8] Bill Tallis, "IChemE Sustainable Development Progress Metrics," Institute of Chemical Engineers,1997.

[9] KPMG, "The KPMG Survey of Corporate Responsibility Reporting 2013," KPMG International, Netherlands,2013.

[10] DJSI, "Dow Jones Sustainability World Index Guide," RebecoSAM,2013.

[11] IChemE. (2002). The Sustainability Metrocs: Sustainable Devolopment Progress Metrics recommended for use in the Process Industries. Available: https://www.icheme.org/communities/special-interest-groups/sustainability/resources/sustainability%20tools.aspx

[12] GRI, "G4 Sustainability Reporting Guidelines: Reporting Pronciples and Standard Disclosures," Global Reporting Initiative,2013.

[13] Calvin Cobb, Darlene Schuster, Beth Beloff, and Dicksen Tanzil, "The AIChE Sustainability Index: The Factors in Detail," *Chemical Engineering Progress,* vol. January 2009, pp. 60-63, 2009.

[14] Ignacio E. Grossmann and Arthur W. Westerberg, "Research challenges in process systems engineering," *AIChE Journal,* vol. 46, pp. 1700-1703, 2000.

[15] Karsten-Ulrich Klatt and Wolfgang Marquardt, "Perspectives for process systems engineering—Personal views from academia and industry," *Computers & Chemical Engineering,* vol. 33, pp. 536-550, 2009.

[16] IgnacioE Grossmann, JoseAntonio Caballero, and Hector Yeomans, "Mathematical programming approaches to the synthesis of chemical process systems," *Korean Journal of Chemical Engineering,* vol. 16, pp. 407-426, 1999.

[17] Bhavik R. Bakshi and Joseph Fiksel, "The quest for sustainability: Challenges for process systems engineering," *AIChE Journal,* vol. 49, pp. 1350-1358, 2003.

[18] Hosoo Kim, Ik Hyun Kim, and En Sup Yoon, "Multiobjective Design of Calorific Value Adjustment Process using Process Simulators," *Industrial & Engineering Chemistry Research,* vol. 49, pp. 2841-2848, 2010/03/17 2010.

[19] A. Aspelund, T. Gundersen, J. Myklebust, M.P. Nowak, and A. Tomasgard, "An optimization-simulation model for a simple LNG process," *Computers & Chemical Engineering,* vol. 34, pp. 1606-1617, 2010.

[20] Vicente Rico-Ramirez, "Representation, Analysis and Solution of Conditional Models in an Equation-Based Envionment," Doctor of Philosophy, Chemical Engineering, Carnegie Mellon University, 1998.

[21] Paul I. Barton, "The Equation Oriented Strategy for Process Flowsheeting," Massachusetts Institute of Technology, Cambridge, MA,2000.

[22] Gerald Jonker and Jan Harmsen, *Engineering for Sustainability: A Practical Guide for Sustainable Design*. Amsterdam: Elsevier, 2012.

[23] Massao Fukushima and Nobuo Yamashita, "Covariance Matrix Adaptation Evolution Strategy for Constrained Optimization Problem," Kyoto University, Kyoto, Japan,2007.

[24] Nikolaus Hansen and Stefan Kern, "Evaluating the CMA Evolution Strategy on Multimodal Test Functions," presented at the 8th International Conference on Parallel Problem Solving from Nature - PPSN VIII, Berlin, 2004.

[25] Ka-Veng Yuen, *Appendix A: Relationship between the Hessian and Covariance Matrix for Gaussian Random Variables*: John Wiley & Sons, Ltd, 2010.

[26] Nikolaus Hansen, Anne Auger, Raymond Ros, Steffen Finck, and Pošík, "Comparing results of 31 algorithms from the black-box optimization benchmarking BBOB-2009," in *Proceedings of the 12th annual conference companion on Genetic and evolutionary computation*, 2010, pp. 1689–1696.

[27] Nikolaus Hansen and Andreas Ostermeier, "Completely Derandomized Self-Adaptation in Evolution Strategies," *Evolutionary Computation,* vol. 9, pp. 159-195, 2001.

[28] Frank Hoffmeister and Thomas Bäck, "Genetic Algorithms and evolution strategies: Similarities and differences," in *Parallel Problem Solving from Nature*. vol. 496, H.-P. Schwefel and R. Männer, Eds., ed: Springer Berlin Heidelberg, 1991, pp. 455-469.

[29] Yossi Borenstein and Alberto Moraglio, *Theory and Principled Methods for the Design of Metaheuristics*: Springer, 2013.

[30] Nikolaus Hansen, Sibylle D. Müller, and Petros Koumoutsakos, "Reducing the Time Complexity of the Derandomized Evolution Strategy with Covariance Matrix Adaptation (CMA-ES)," *Evolutionary Computation,* vol. 11, pp. 1-18, 2003.

[31] N. Hansen and A. Ostermeier, "Adapting arbitrary normal mutation distributions in evolution strategies: the covariance matrix adaptation," in *Proceedings of IEEE International Conference on Evolutionary Computation*, 1996, pp. 312-317.

[32] Nikolaus Hansen, "The CMA Evolution Strategy: A Comparing Review," in *Towards a New Evolutionary Computation*. vol. 192, J. Lozano, P. Larrañaga, I. Inza, and E. Bengoetxea, Eds., ed: Springer Berlin Heidelberg, 2006, pp. 75-102.

[33] Nikolaus Hansen. (2011). *The CMA Evolution Strategy: A Tutorial*. Available: https://www.lri.fr/~hansen/cmaesintro.html

[34] Christian Spieth, Rene Worzischek, and Felix Streichert, "Comparing evolutionary algorithms on the problem of network inference," in *Proceedings of the 8th annual conference on Genetic and evolutionary computation*, Seattle, Washington, USA, 2006, pp. 305-306.

[35] Steffen Finck, Nikolaus Hansen, Raymond Ros, and Anne Auger. (2013). *Real-Parameter Black-Box Optimization Benchmarking 2010: Presentation of the Noiseless Functions*. Available: http://coco.gforge.inria.fr/

[36] Nikolaus Hansen, Raymond Ros, Nikolas Mauny, Marc Schoenauer, and Anne Auger, "Impacts of invariance in search: When CMA-ES and PSO face ill-conditioned and non-separable problems," *Applied Soft Computing,* vol. 11, pp. 5755-5769, 12// 2011.

[37] Nikolaus Hansen, Anne Auger, Steffen Finck, and Raymond Ros. (2013). Real-Parameter Black-Box Optimization Benchmarking: experimental setup. Available: http://coco.gforge.inria.fr/doku.php?id=bbob-2013-downloads

[38] SooHyoung Choi and Vasilios Manousiouthakis, "Global optimization methods for chemical process design: Deterministic and stochastic approaches," *Korean Journal of Chemical Engineering,* vol. 19, pp. 227-232, 2002/03/01 2002.

[39] Zbigniew Michalewicz, Dipankar Dasgupta, Rodolphe G. Le Riche, and Marc Schoenauer, "Evolutionary algorithms for constrained engineering problems," *Computers & Industrial Engineering,* vol. 30, pp. 851-870, 9// 1996.

[40] AspenTech, *Aspen HYSYS Customization Guide*: Aspen Technology, Inc., 2011.

[41] Havard Devold, *Oil And Gas Production Handbook: An Introduction To Oil And Gas Production*: ABB ATPA Oil and Gas, 2006.

[42] H. K. Abdel-Aal, Mohamed Aggour, and M. A. Fahim, *Petroleum and Gas Field Processing*. U.S.A.: CRC Press, 2003.

[43] Elaine Su-Qin Lee and G. P. Rangaiah, "Optimization of Recovery

Processes for Multiple Economic and Environmental Objectives," *Industrial & Engineering Chemistry Research,* vol. 48, pp. 7662-7681, 2009/08/19 2009.

[44] Grzegorz Boczkaj, Andrzej Przyjazny, and Marian Kamiński, "New Procedures for Control of Industrial Effluents Treatment Processes," *Industrial & Engineering Chemistry Research,* 2014.

[45] "Compilation of air pollutant emission factors," vol. Volume I: Stationary point and area sources, U. S. E. P. Agency, Ed., 5th ed, 1995.

[46] Djebri Mourad, Otmanine Ghazi, and Bentahar Noureddine, "Recovery of flared gas through crude oil stabilization by a multi-staged separation with intermediate feeds: A case study," *Korean Journal of Chemical Engineering,* vol. 26, pp. 1706-1716, 2009/11/01 2009.

[47] API, "Toward a consistent methodology for estimating greenhouse gas emissions from oil and natural gas industry operations," American Petroleum Institute, U.S.A.,2002.

[48] Yu C. Pan, S. Joe Qin, Phi Nguyen, and Michael Barham, "Hybrid Inferential Modeling for Vapor Pressure of Hydrocarbon Mixtures in Oil Production," *Industrial & Engineering Chemistry Research,* vol. 52, pp. 12420-12425, 2013/09/04 2013.

[49] Ken E. Arnold and Maurice Stewart, *Surface Production Operations, Volume 1 : Design of Oil Handling Systems and Facilities*, 3rd ed.: Gulf Professional Publishing, 2007.

[50] Ik Hyun Kim, Seungkyu Dan, Hosoo Kim, Hung Rae Rim, Jong Min Lee, and En Sup Yoon, "Simulation-Based Optimization of Multistage Separation Process in Offshore Oil and Gas Production Facilities," *Industrial & Engineering Chemistry Research,* vol. 53, pp. 8810-8820, 2014/05/28 2014.

[51] John M. Campbell, *Gas conditioning and processing*. Norman, Oklahoma: Campbell Petroleum Series, 1976.

[52] G. V. Chilingarian, *Surface Operations in Petroleum Production, I*: Elsevier Science, 1987.

[53] Kenneth Whinery and John Campbell, "A Method for Determining Optimum Second Stage Pressure in Three Stage Separation," *Journal of Petroleum Technology,* vol. 10, pp. 53-54, 1958.

[54] Brian Boyer and Steve O'Connell, "Optimize Separator Operating Pressures to Reduce Flash Losses," presented at the 2005 SPE/EPA/DOE Exploration and Production Environmental Conference, 2005.

[55] Alireza Bahadori, Hari B. Vuthaluru, and Saeid Mokhatab, "Optimizing separator pressures in the multistage crude oil production unit," *Asia-Pacific Journal of Chemical Engineering,* vol. 3, pp. 380–386, 2008.

[56] Øyvind Widerøe Kylling, "Optimizing separator pressure in a multistage crude oil production plant," M.S., Norwegian University of Science and Technology, 2009.

[57] Francis S. Manning and Richard E. Thompson, *Oilfield Processing, Vol. 2: Crude Oil*. Tulsa, Oklahoma: Pennwell, 1995.

[58] Mahsakazemi, "Optimization of Oil and Gas Multi Stage Separators Pressure to Increase Stock Tank Oil," *Oriental Journal of Chemistry,* vol. 27, pp. 1503-1508, 2011.

[59] William C. Lyons, *Standard Handbook of Petroleum and Natural Gas Engineering*: Gulf Professional Publishing, 2004.

[60] GPSA, *GPSA Engineering Data Book*, 12th ed. Tulsa, Oklahoma: Gas Processors Suppliers Association, 2004.

[61] AspenTech, *Aspen HYSYS Upstream Operations Guide*: Aspen

Technology, Inc., 2011.

[62] Gilbert Strang, *Introduction to Linear Algebra*, 4th ed. Wellesley MA: Wellesley-Cambridge Press, 2009.

[63] Warren D. Seider, J. D. Seader, Daniel R. Lewin, and Soemantri Widagdo, *Product and Process Design Principles: Synthesis, Analysis and Design*, 3rd ed. U.S.A.: Wiley, 2008.

[64] Gael D. Ulrich and Palligarnai T. Vasudevan, "Predesign for Pollution Prevention and Control," *Chemical Engineering Progress,* vol. June 2007, pp. 53-60, 2007.

[65] Jamin Koo, Seunghyok Kim, Hyosuk Kim, Young-Hun Kim, and EnSup Yoon, "A systematic approach towards accident analysis and prevention," *Korean Journal of Chemical Engineering,* vol. 26, pp. 1476-1483, 2009/11/01 2009.

[66] W. So, Y. H. Kim, C. J. Lee, D. Shin, and E. S. Yoon, "Optimal layout of additional facilities for minimization of domino effects based on worst-case scenarios," *Korean Journal of Chemical Engineering,* vol. 28, pp. 656-666, 2011.

[67] Young-Hun Kim, Won So, Dongil Shin, and EnSup Yoon, "Safety distance analysis of dimethylether filling stations using a modified individual risk assessment method," *Korean Journal of Chemical Engineering,* vol. 28, pp. 1322-1330, 2011/06/01 2011.

[68] Kyungtae Park, Jamin Koo, Dongil Shin, Chang Jun Lee, and EnSup Yoon, "Optimal multi-floor plant layout with consideration of safety distance based on mathematical programming and modified consequence analysis," *Korean Journal of Chemical Engineering,* vol. 28, pp. 1009-1018, 2011/04/01 2011.

[69] Jaedeuk Park, Younghee Lee, Yi Yoon, Sougboum Kim, and Il Moon,

"Development of a web-based emergency preparedness plan system in Korea," *Korean Journal of Chemical Engineering,* vol. 28, pp. 2110-2115, 2011/11/01 2011.

[70] Namjin Jang, Seungkyu Dan, Dongil Shin, Gibaek Lee, and En Sup Yoon, "The Role of Process Systems Engineering for Sustainability in the Chemical Industries," *Korean Chem. Eng. Res.,* vol. 51, pp. 221-225, 2013.

[71] J. Suokas and R. Kakko, "Safety analysis, Risk analysis, Risk management," in *Quality Management of Safety and Risk Analysis*, J. Soukas and V. Rouhiainen, Eds., ed Amsterdam: Elsevier, 1993, pp. 9-18.

[72] CCPS, *Guidelines for Hazard Evaluation Procedures*, 3rd ed. New York: Center for Chemical Process Safety of American Institute of Chemical Engineers, 2008.

[73] Anna-Mari Heikkilä, *Inherent Safety in Process Plant Design: An Index-Based Approach*. Espoo, Finland: Technical Research Centre of Finland, 1999.

[74] Chan T. Leong and Azmi Mohd Shariff, "Inherent safety index module (ISIM) to assess inherent safety level during preliminary design stage," *Process Safety and Environmental Protection,* vol. 86, pp. 113-119, 3// 2008.

[75] J. R. Taylor, *Risk Analysis for Process Plant, Pipelines and Transport*. U.K.: E&FN Spon, 1994.

[76] Azmi Mohd Shariff, Risza Rusli, Chan T. Leong, V. R. Radhakrishnan, and Azizul Buang, "Inherent safety tool for explosion consequences study," *Journal of Loss Prevention in the Process Industries,* vol. 19, pp. 409-418, 9// 2006.

[77] Raymond A. Freeman, "CCPS guidelines for chemical process quantitative risk analysis," *Plant/Operations Progress,* vol. 9, pp. 231-235,

1990.

[78] Sam Mannan, *Lees' Loss prevention in the process industries: Hazard identification, assessment and control*: Elsevier Butterworth-Heinemann, 2004.

[79] Azmi Mohd Shariff and Chan T. Leong, "Inherent risk assessment—A new concept to evaluate risk in preliminary design stage," *Process Safety and Environmental Protection,* vol. 87, pp. 371-376, 11// 2009.

[80] Norwegian Technology Centre, "NORSOK STANDARD P-100 : Process systems," Standards Norway,2001.

[81] Norwegian Technology Centre, "NORSOK STANDARD Z-013 : Risk and emergency preparedness analysis," Standards Norway,2001.

[82] Norwegian Technology Centre, "NORSOK STANDARD S-001 : Technical safety," Standards Norway,2008.

[83] Norwegian Technology Centre, "NORSOK STANDARD N-001 : Integrity of offshore structures," Standards Norway,2010.

[84] Gadhiraju Venkatarathnam, *Cryogenic mixed refrigerant processes*: Springer, 2008.

[85] Øyvind Eckhardt, "Evaluation of Natural Gas liquefaction Processes for Floating Applications Offshore," Master of Science, Department of Energy and Process Engineering, Norwegian University of Science and Technology, Feb 2010.

[86] Sultan Seif Pwaga, "Sensitivity Analysis of Proposed LNG Liquefaction Processes for LNG FPSO," Master of Science, Department of Energy and Process Engineering, Norwegian University of Science and Technology, July 2011.

[87] Nipen M. Shah, Andrew F. A. Hoadley, and G. P. Rangaiah, "Inherent

Safety Analysis of a Propane Precooled Gas-Phase Liquified Natural Gas Process," *Industrial & Engineering Chemistry Research,* vol. 48, pp. 4917-4927, 2009/05/20 2009.

[88] John Lowell Woodward, *Estimating the flammable mass of a vapor cloud*: Center for Chemical Process Safety of the American Institute of Chemical Engineers, 1999.

[89] CEPPO, "Risk Management Program Guidance for Offsite Consequence Analysis," Chemical Emergency Preparedness and Prevention Office of U.S. EPA,1999.

[90] Netherland Organization for Applied Scientific Research TNO Bureau for Industrial Safety, *Methods for the Calculation of Physical Effects: Due to Releases of Hazardous Materials (liquids and Gases) : Yellow Book*. The Hague, the Netherlands: Committee for the Prevention of Disasters, 1997.

[91] "Control of Industrial Major Accident and Hazard (CIMAH) Report for Malaysia LNG Tiga SDn. Bhd.," Professional Loss Control, Kuala Lumpur,2003.

[92] Azmi Mohd Shariff, Chan T. Leong, and Dzulkarnain Zaini, "Using process stream index (PSI) to assess inherent safety level during preliminary design stage," *Safety Science,* vol. 50, pp. 1098-1103, 4// 2012.

요 약 (국문초록)

공분산행렬 적응형 진화알고리즘을 이용한 지속가능성 최적화를 위한 공정 설계

화학공정의 기초설계는 물질수지와 열수지 계산을 기초로 공정의 경제성을 확보하고 주어진 조건 내에서 원하는 제품을 생산 가능하도록 한다. 이 단계를 통해 공정은 사용될 물질과 반응, 설비의 구조와 운전 조건 등이 결정되기 때문에 이후 바꿀 수 없는 고유한 특성을 갖게 된다. 때문에 공정의 지속가능성을 확보하기 위해서는 기초설계 단계에서부터 지속가능성의 수치화를 통해 최적화하는 것이 필요하다.

이에 본 논문은 수치화된 지속가능성을 공정 최적화에 통합하여 풀이하는 방법론을 제안하였다. 공정의 모델링은 화학공정의 설계 및 분석을 위해 순차적 모듈 방식의 상용모사기를 이용하여 편리성과 신뢰성을 동시에 확보하였다. 순차적 모듈 방식의 공정모사기 내 공정모델은 도함수를 구하여 결정론적 방법론을 통해 최적화에 이용하기 어렵고 공정 내 하나 이상의 설계변수와 상호작용하는 공정조건 또는 설계사양을 만족시키기 어려워 확률론 기반의 공분산행렬 적응형 진화알고리즘(CMA-ES)을 도입하였다. CMA-ES는 기존의 확률론 기반의 최적화 방법론들보다 정확성과 풀이시간이 획기적으로 개선한 방법론으로 1) 사용자가 최적화를 수행하기

위해 제공해야 하는 초기 설정값이 상대적으로 거의 없고, 2) 실제 공정의 구조와 해석이 복잡하여 수학적 모델의 명쾌한 풀이가 어려운 모델에도 적용가능하며, 3) 지역최적해가 많은 다봉성 비볼록 함수나 불연속적인 의사결정 변수가 포함된 경우에 대해서도 적용이 가능하고, 4) 설계변수가 많은 다변수 최적화 문제도 빠르게 풀어낼 수 있다는 장점이 있어, 본 연구에서 제안된 방법론의 우수성을 더 하였다.

공정 기초설계 단계에서 공정모사기를 이용한 지속가능성 최적화 문제의 해결을 위해 제안된 통합적 풀이 방법론은 공정 모델의 해석을 위한 공정모사기 내에 존재하는 내부루프와 경제성 및 지속가능성을 최적화하기 위한 외부루프가 존재하는 중첩루프 구조를 갖는다. 내·외부 루프 풀이를 위한 시간이 많이 걸리는 중첩루프의 한계는 1) 높은 정확성과 적은 반복계산을 통해 빠르게 최적해에 수렴 가능한 CMA-ES를 사용하고, 2) 상대적으로 많은 계산시간을 요하는 내부루프인 공정모사기의 불필요한 계산과 오류를 발생시키는 원인을 이전에 차단하여 회피하는 채택기각방법론을 적용하여 전체 계산시간은 줄이고 설계변수 탐색 영역은 넓혀 극복할 수 있도록 하였다.

본 연구를 통해서 제안된 방법론은 실제 공정 설계 문제에 적용하여 그 유용성과 효율성을 입증하였다. 첫째로 해양 원유 생산 시설의 특성상

반드시 고려해야 하지만 기존의 방법론의 한계로 체계적으로 풀이하지 못하던 대기 및 수질 오염 관련 환경적 요소를 경제성과 함께 고려하여, 환경 친화적 해양설비의 설계가 가능하도록 하였다. 둘째로 사고 위험성으로 인해 실제 공정 도입에 한계를 갖고 있는 해양 천연가스 액화 플랫폼의 혼합냉매 이용을 위해 내재적 폭발 위험성을 분석하여 수치화하는 방법론을 도입하여 경제성 평가와 통합함으로써 상호 충돌하는 목적함수 사이의 정량적 관계를 효과적으로 나타내고 내재적으로 안전한 공정을 위한 설계변수를 결정하여 의사결정에 이용되도록 하였다.

본 연구를 통해 제안된 방법론은 최근 부각되고 있는 지속 가능 발전을 위한 공정 설계가 가능하게 하고, 이를 수치적으로 최적화에 이용함으로써 의사결정 지원 시스템을 위한 학문적·실용적 가치를 보여주었으며, 환경 및 공정안전성을 초기 설계에 반영함으로 인해 이 후 상세설계 및 운전·생산 단계에서 불확실성으로 인해 발생할 추가 비용을 최소화하는데 주된 기여를 기대할 수 있다.

주요어 : 지속가능성, 공정설계, 공정모사, 확률 기반 최적화, 해양플랫폼

학 번 : 2009-30239 성 명 : 김 익 현